

Biophysical Properties, Thermal Stability, and Functional Impact of 8-oxo-7,8-dihydroguanine on Oligonucleotides of RNA. A Study of Duplex, Hairpins, and the Aptamer for preQ₁ as Models

Yu Jung Choi,[†] Krzysztof S. Gibala,[†] Tewoderos Ayele, Katherine Van Deventer and Marino J.

E. Resendiz*

Department of Chemistry, University of Colorado Denver, Science Building 1151
Arapahoe St, Denver, CO 80204

[*Marino.resendiz@ucdenver.edu](mailto:Marino.resendiz@ucdenver.edu)

[†] These authors contributed in the same amount to this work.

Supporting Information Index:

| Page | Contents: |
|------------|---|
| S3-15..... | Experimental details and figures pertaining to the synthesis of phosphoramidite 8-oxoG – Figures S1 - S10 . |
| S16..... | Figure S11 . ¹ H NMR and ³¹ P NMR of phosphoramidite 8-OMeG . |
| S17..... | Figure S12 . MALDI-TOF MS of 1, 2, 3, and 4 . |
| S18..... | Figure S13 . MALDI-TOF MS of 5, 6, 7, and 8 . |
| S19..... | Figure S14 . MALDI-TOF MS of 10, 11, and 12 . |
| S20..... | Figure S15 . MALDI-TOF MS of 13, 15, and 16 . |
| S21..... | Figure S16 . MALDI-TOF MS of 17, 17-OMe, 18, 19, and 20 . |
| S22..... | Figure S17 . MALDI-TOF MS of 21, 22, and 23 . |
| S23..... | Figure S18/S19 . CDs and melts of strands 1&1:5 and 2&2:5 . |
| S24..... | Figure S20/S21 . CDs and melts of strands 3&3:5 and 4&4:5 . |
| S25..... | Figure S22/S23/S24 . CDs and melts of strands 10, 1:6, and 2:7 . |
| S26..... | Figure S25/S26/S27 . CDs and melts of strands 1:6, 2:6, and 3:6 . |
| S27..... | Figure S28/S29/S30 . CDs and melts of strands 4:6, 8, and 9 . |
| S28..... | Figure S31/S32/S33 . CDs and melts of strands 10, 11, and 12 . |

S29.....**Figure S34/S35/S36.** CDs and melts of strands **13, 14,** and **15.**

S30.....**Figure S37/S38/S39.** CDs and melts of strands **16, 17',** and **17.**

S31.....**Figure S40/S41/S42.** CDs and melts of strands **17-OMe, 18,** and **19.**

S32.....**Figure S43/S44/S45.** CDs and melts of strands **20, 21,** and **22.**

S33.....**Figure S46.** CD and melt of strand **23.**

S34.....**Figure S47.** Mobility shift assays for **17** at varying concentrations to show **17→17'** transformation.

Figure S48. Mobility shift assays for the unimolecular secondary structure of **17-OMe, 18-20, 13, 14,** and **16, 8-10.**

S35.....**Figure S49.** UV-vis of guanosine and 8-oxoG.

S35.....Synthesis of phosphoramidite **8-OMeG.**

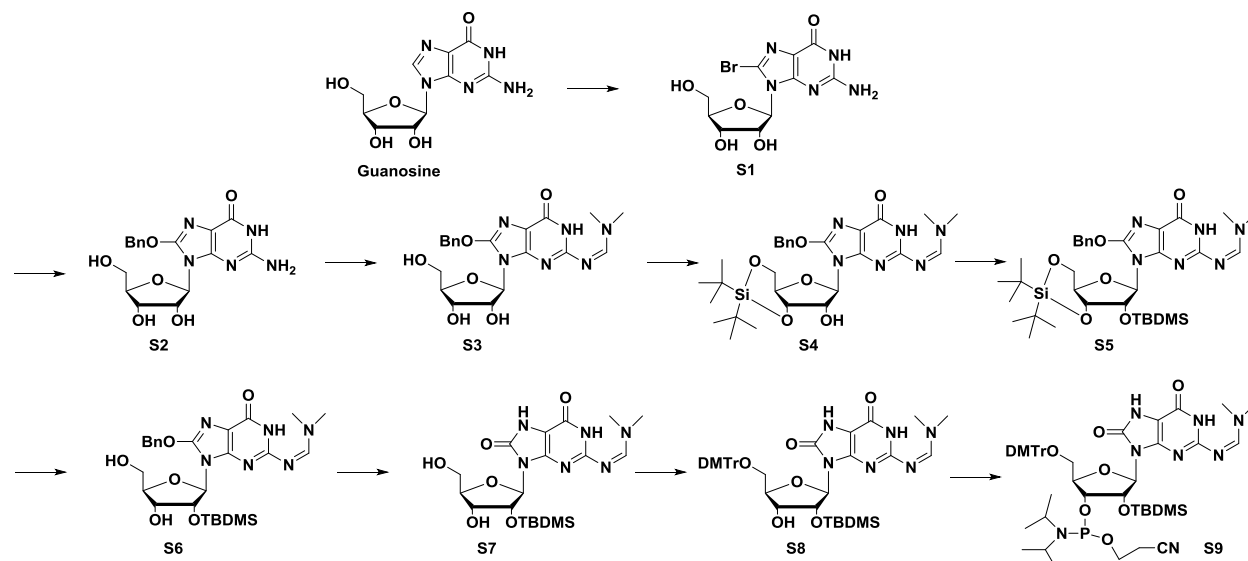
S36.....**Figure S50.** Reference for the synthesis of phosphoramidite **8-OMeG.**

S37.....**Figure 51.** T_m measurements of strands **1:5, 2:5, 3:5, 4:5, 1:7** and **2:7** recorded at 270 nm

S38.....**Figure 52.** T_m measurements of strands **1:6, 2:6, 3:6,** and **4:6** recorded at 270 nm

S39.....**Figure 53.** T_m measurements of strands **1:5, 2:5, 3:5,** and **4:5, 1:7** OD recorded

S40.....References



8-bromoguanosine (S1)¹

Guanosine (13.0 g, 45.92 mmol) was dissolved in 350 mL H₂O and 2.6 mL (101.0 mmol) Br₂. The mixture was stirred for 2 h followed by addition of NaHSO₃ until a pale yellow suspension was obtained. Following vacuum filtration, the solid cake was recrystallized from a 1:1 MeOH/H₂O solution (400 mL). The mixture was filtered and washed with diethyl ether, yielding 15.0 g (90.2 %) of compound **S2**.

8-benzyloxyguanosine (S2)¹

Sodium benzyloxide was prepared by adding sodium metal (4.6 g, 200.1 mmol) to benzyl alcohol (130 mL, 14058.2 mmol), and stirring for 12 h followed by addition of DMSO (85 mL). In a separate flask, **S2** (15 g, 42.8 mmol) was dissolved in 85 mL DMSO and stirred for 15 min. The two solutions were combined and placed in a 65 °C oil bath for 4.5 h. The reaction was neutralized using glacial acetic acid. The slurry was placed in diethyl ether and stirred for 5 min, then decanted. Acetone was placed into the slurry and stirred for 5 min. After vacuum filtration, the solid was stirred in DCM and filtered. The remaining solid was dried under reduced pressure and re-crystallized in 500 mL of a 1:1 EtOH/H₂O solution to yield **S2** in the form of a white solid (16.1 g, 41.1 mmol, 96.0 %) ¹H NMR(DMSO-d₆) δ 7.47-7.38 (m, 5H), 5.62 (d, *J*= 6, 1H), 5.40 (s, 2H), 4.74 (t, *J*=12, 1H), 3.99 (t, *J*=12, 1H), 3.77 (q, *J*=12, 1H).

2-*N*-(dimethyl formamide)-8-benzyloxyguanosine (S3)

N,N-dimethylformamide dimethyl acetal (16.3 mL, 122.5 mmol) was added to a solution of **S3** (16.1 g, 41.1 mmol) in 161 mL DMF and stirred at 45 °C for 1.5 h. The mixture was concentrated under reduced pressure and re-dissolved in ethanol (20 mL). Following concentration under reduced pressure, **S3** was obtained in the form of a white foam (11.3 g, 25.4 mmol, 62.0 %). ¹H NMR(DMSO-d₆) δ 8.46 (s, 1H), 7.51-7.37 (m, 5H), 5.71 (d, *J*=6, 1H), 5.45 (s, 2H), 4.78 (t, *J*=12, 1H), 4.07 (t, *J*=12, 1H), 3.81 (q, *J*=12, 1H), 3.53 (m, 1H), 3.14 (s, 3H), 3.02 (s, 3H); ¹³C NMR (DMSO) δ 157.7, 156.8, 156.5, 151.7, 148.8, 135.8, 128.5, 128.3, 128.1, 114.3, 86.5, 85.2, 71.0, 70.8, 70.5, 62.0, 40.7, 34.6; IR 3234, 2926, 1674, 1331 cm⁻¹. HRMS *m/z* calculated for C₂₀H₂₅N₆O₆(M⁺+ H), 445.1830, observed *m/z* = 445.1845.

2-*N*- (dimethyl formamide)- 3',5'-*O*-bis-(*t*-butylsilyl)-8-benzyloxyguanosine (S4)

Nucleoside **S3** (1.2 g, 2.7 mmol) was azeotropically dried over pyridine (10 mL). The solid was then dissolved in DMF (10 mL) and cooled to 0 °C followed by addition of di-*tert*-butylsilyl bis(trifluoromethanesulfonate) (1.75 mL, 5.4 mmol). The solution was stirred for 1 h and imidazole (0.9 g, 13.2 mmol) was added at once with further stirring (5 min). The solution was mixed with aq. NH₄Cl (30 mL, 0.01M) and extracted using ethyl acetate (10 mL x3). The organic residues were dried over brine and sodium sulfate, concentrated under reduced pressure and purified using column chromatography (1:1 DCM/EtOAc, 100 % DCM, 0-4 % MeOH/DCM) to afford nucleoside **S4** in the form of a white foam. (1.25 g, 2.1 mmol, 77 %). ¹H NMR(DMSO-d₆) δ 11.37 (s, 1H), 8.47 (s, 1H), 7.39 (m, 5H), 5.73 (d, J=12, 1H), 5.43 (s, 2H), 4.65 (t, J=12, 1H), 4.27 (m, 1H), 4.21(m, 1H), 3.77 (m, 1H), 3.15 (s, 3H), 3.03 (s, 3H), 1.01-0.84 (m, 18H); ¹³C NMR (CDCl₃) δ 157.8, 157.4, 156.2, 152.1, 149.3, 135.2, 128.9, 128.9, 128.8, 115.0, 88.2, 75.9, 74.4, 72.4, 72.3, 67.4, 41.5, 35.3, 27.4, 27.3, 22.6, 20.4; IR 2934, 2858, 1677, 1529,1338 cm⁻¹. HRMS m/z calculated for C₂₈H₄₁N₆O₆Si(M⁺+ H), 585.2851, observed m/z = 585.2849.

2-*N*- (dimethyl formamide)-2'-*O*-(*t*-butyldimethylsilyl)- 3',5'-*O*-bis-(*t*-butylsilyl)-8-benzyloxyguanosine (S5)

Nucleoside **S4** (1.12 g, 1.9 mmol) and imidazole (3.52 g, 51.7 mmol) were azeotropically dried over pyridine (3 mL). The obtained solids were then dissolved in DMF (10 mL) followed by addition of *tert*-butyldimethylsilyl trifluoromethanesulfonate (8.75 mL, 38.1 mmol) with stirring over 12 h at rt. Additional 4.35 mL (18.9 mmol) of the bis-triflate was added and stirred for additional 1 h. Saturated NH₄Cl was added and the organics were extracted over ethyl acetate (10 mL x3) with drying over brine and sodium sulfate. Purification using column chromatography (1:1 DCM/EtOAc, 100 % DCM, 0-2% MeOH/DCM) yielded **S5** in the form of a white foam (0.76 g, 1.1 mmol, 57 %). ¹H NMR(DMSO-d₆) δ 11.41 (s, 1H), 8.42 (s, 1H), 7.43-7.40 (m, 5H), 5.74 (s, 1H), 5.44 (s, 2H), 4.65 (s, 1H), 4.29 (m, 2H), 3.80 (m, 1H), 3.11 (s, 3H), 3.02 (s, 3H), 1.02-0.80 (m, 27H), 0.03 (m, 6H); ¹³C NMR (CDCl₃) δ 157.7, 157.3, 156.0, 152.1, 149.1, 135.3, 128.8, 115.3, 90.3, 75.8, 74.3, 67.6, 41.4, 35.3, 27.5, 27.2, 25.9, 25.8, 22.6, 20.5, 18.1, -3.54, -4.30, -5.19; IR 2933, 2858, 1679, 1504,1336 cm⁻¹; HRMS m/z calculated for C₃₄H₅₅N₆O₆Si₂(M⁺+ H), 699.3716, observed m/z = 699.3726.

2-*N*- (dimethyl formamide)-2'-*O*-(*t*-butyldimethylsilyl)-8-benzyloxyguanosine (S6)

THF (8 mL) was added to a flask containing compound **S5** (0.45 g, 0.64 mmol) and cooled to 0 °C. Triethylamine trihydrofluoride (0.3 mL, 1.8 mmol) was dissolved in pyridine (0.5 mL) and added dropwise over a period of 20 min with stirring at 0° C. The reaction mixture was neutralized with slow addition of 15 % NaHCO₃ (10 mL) at 0 °C. Water (10 mL) was then added and the mixture was extracted with EtOAc (10 mL x3) and dried over brine and sodium sulfate. Column chromatography (0-5 % MeOH/EtOAc) afforded residue **S6** in the form of a white foam (0.17 g, 0.31 mmol, 48 %). ¹H NMR(DMSO-d₆) δ 11.49 (s, 1H), 8.52 (s, 1H), 7.57-7.51 (m, 5H), 5.82 (d, J=6, 1H), 5.55 (s, 2H), 4.99 (m, 1H), 4.17 (m, 1H), 3.98 (m, 1H), 3.64 (m, 1H), 3.23 (s, 3H), 3.13 (s, 3H), 0.83 (s, 9H), 0.03 (m, 6H); ¹³C NMR (CD₃OD) δ 159.3, 158.2, 154.1, 150.9, 136.5, 129.8, 129.7, 116.0, 88.5, 87.4, 74.6, 73.1, 72.6, 63.6, 61.5, 41.4, 35.2, 26.1,

20.9, 19.0, 14.5, -4.80, -5.09; IR 2928, 2856, 2357, 1662, 1619, 1339 cm^{-1} ; HRMS m/z calculated for $\text{C}_{26}\text{H}_{39}\text{N}_6\text{O}_6\text{Si}(\text{M}^+ + \text{H})$, 559.2695, observed $m/z = 559.2718$.

2-*N*-(dimethyl formamide)-2'-*O*-(*t*-butyldimethylsilyl)-8-hydroxy-7,8-dihydroguanosine (S7)

Residue **S6** (0.17 g, 0.31 mmol) and Pd/C (0.08 g, 0.75 mmol) were placed in a pressure chamber and suspended in EtOH (2.5 mL). The chamber was filled with H_2 (60 psi) and left stirring for 45 min. The mixture was then filtered through Celite[®] 545 and washed with EtOH (3 mL x3). Drying under reduced pressure yielded compound **S7** in the form of a white foam (0.13 g, 0.27 mmol, 87 %). ^1H NMR(CD_3OD) δ 8.59 (s, 1H), 5.94 (d, 1H), 5.12 (, 1H), 4.33 (m, 1H), 4.11 (m, 1H), 3.88-3.71 (dd, 2H), 3.22 (s, 3H), 3.14 (s, 3H), 0.88 (s, 9H), 0.06 (s, 3H), -0.01 (s, 3H); ^{13}C NMR (CD_3OD) δ 159.5, 158.5, 154.2, 148.5, 103.9, 87.6, 87.1, 73.8, 72.8, 63.7, 41.5, 35.3, 26.2, 19.0, -4.75, -4.99; IR 2929, 2857, 1678, 1539, 1342 cm^{-1} ; HRMS m/z calculated for $\text{C}_{19}\text{H}_{55}\text{N}_6\text{O}_6\text{Si}(\text{M}^+ + \text{H})$, 469.2225, observed $m/z = 469.2215$.

2-*N*-(dimethyl formamide)-2'-*O*-(*t*-butyldimethylsilyl)- 5'-*O*-(4,4'-dimethoxytrityl)-8-hydroxy-7,8-dihydroguanosine (S8)

Compound **S7** (0.20 g, 0.42 mmol) was azeotropically dried over pyridine (1 mL), and re-dissolved in pyridine (4mL). The solution was cooled to 0 °C followed by addition of 4,4'-dimethoxytriphenylmethyl chloride (0.166 g, 0.49 mmol) and stirring for 12 h with slow warming to r.t. The yellow solution was diluted with 15 % NaHCO_3 (10 mL) and extracted with ethyl acetate (7 mL x3) followed by drying over brine and sodium sulfate. Column chromatography (0- 5% MeOH/DCM) produced protected nucleoside **S8** in the form of a white foam (0.12 g, 0.16 mmol, 38 %). ^1H NMR(CDCl_3) δ 8.34 (s, 1H), 7.38-6.72 (m, 13H), 5.82 (d, 1H), 5.02 (s, 1H), 4.42 (s, 1H), 3.94 (s, 1H), 3.68 (s, 6H), 3.34 (s, 2H), 2.92 (s, 3H), 2.79 (s, 3H), 0.84 (s, 9H), 0.01 (m, 6H); ^{13}C NMR (CDCl_3) δ 158.4, 156.2, 153.1, 152.2, 149.7, 147.2, 145.0, 136.2, 136.1, 130.2, 128.3, 127.7, 113.1, 113.0, 103.2, 86.6, 86.0, 83.0, 72.7, 71.0, 55.2, 41.2, 35.0, 25.8, 18.1, -4.64, -5.01; IR 2857, 2361, 1673, 1627, 1508 cm^{-1} ; HRMS m/z calculated for $\text{C}_{40}\text{H}_{50}\text{N}_6\text{O}_8\text{NaSi}(\text{M}^+ + \text{H})$, 793.3352, observed $m/z = 793.3346$

2-*N*-(dimethyl formamide)-2'-*O*-(*t*-butyldimethylsilyl)- 3'-*O*-[(2-ethylcyano-*N,N*-diisopropylphosphoramidite)-5'-*O*-(4,4'-dimethoxytrityl)-8-hydroxy-7,8-dihydroguanosine (S9)

Nucleoside **S8** (0.12 g, 0.16 mmol) was azeotropically driven over pyridine (1 mL), and dissolved in anhydrous DCM (1 mL). Anhydrous DIPEA (0.08 mL, 0.47 mmol) and 2-cyanoethyl-*N,N*-diisopropylchlorophosphoramidite (0.07 mL, 0.31 mmol) were added and stirred for 1 hr. The solution was added to a flask containing 20% NaHCO_3 and extracted with DCM (2 mL x 3). The organics were dried over brine and sodium sulfate. Purification using column chromatography (0-3% MeOH/DCM) yielded phosphoramidite **S9** in the form of a white foam (0.12 g, 0.12 mmol, 77%). ^1H NMR(CDCl_3) δ 8.46 (s, 1H), 7.46-6.77 (m, 13H), 5.91 (d, 1H), 5.15 (s, 1H), 4.50 (s, 1H), 3.23 (s, 1H), 3.76 (s, 6H), 3.74-2.61 (m, 8H), 3.03 (s, 3H), 2.93-2.82 (d, 3H), 2.61 (m, 1H), 1.15-1.04 (m, 12H), 0.84 (s, 9H), 0.05 (s, 3H), -0.03 (m, 3H); ^{31}P NMR(CDCl_3) δ 149.7, 148.9. HRMS m/z calculated for $\text{C}_{49}\text{H}_{68}\text{N}_8\text{O}_9\text{PSi}(\text{M}^+ + \text{H})$, 971.4616, observed $m/z = 971.4567$.

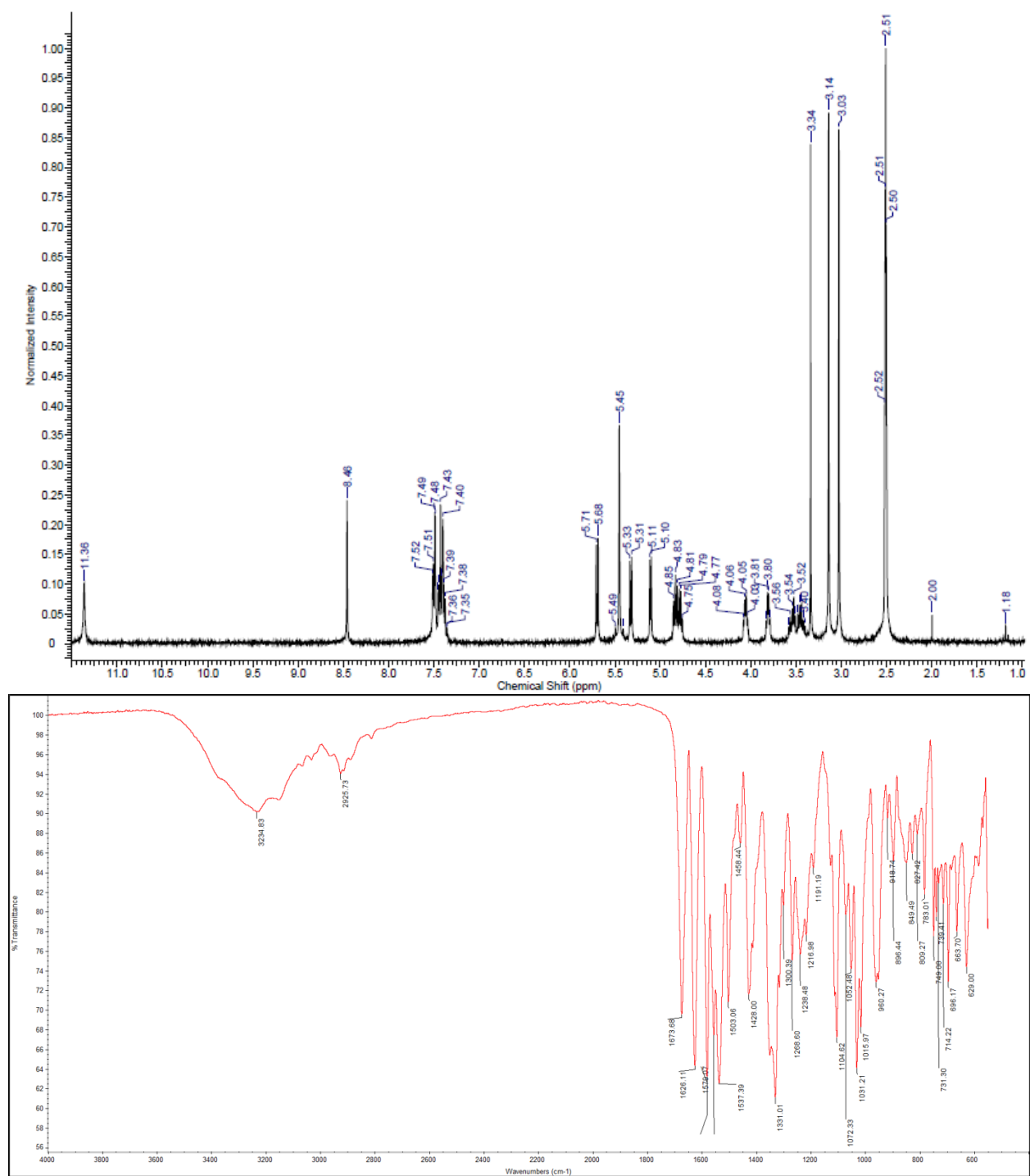


Figure S1. ^1H NMR (top) and IR (bottom) of compound **S3**.

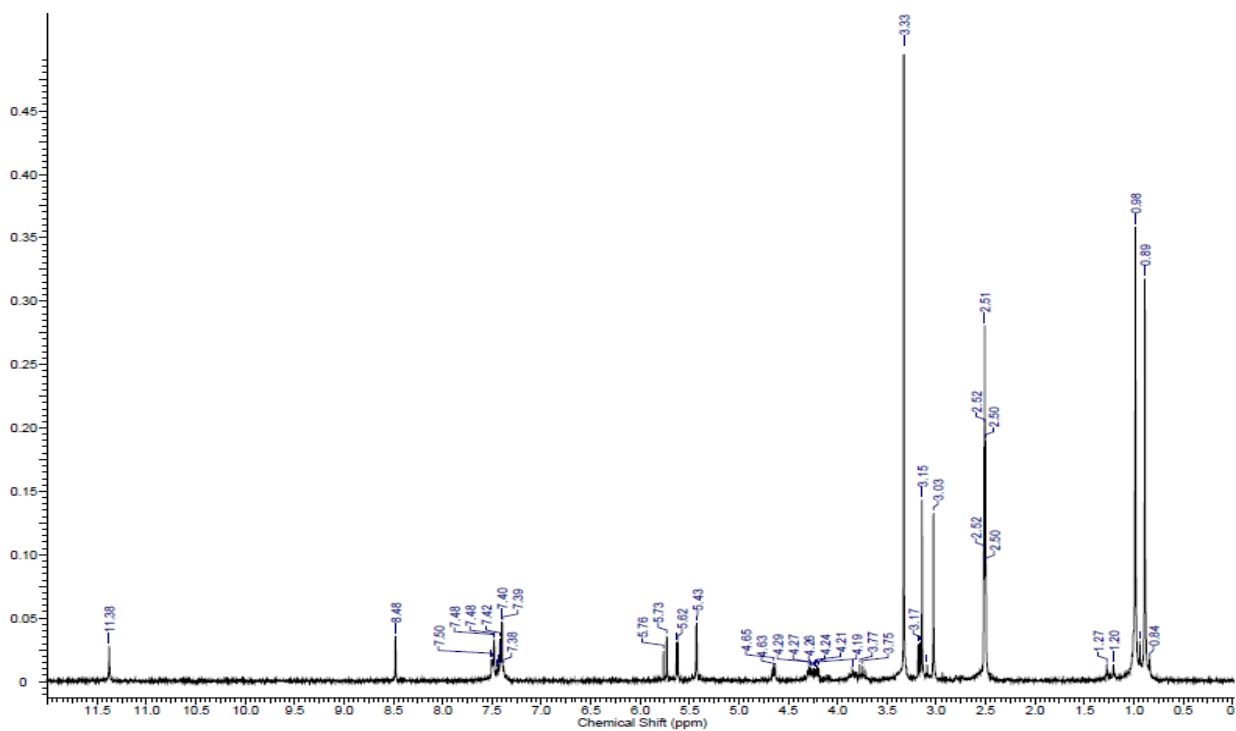
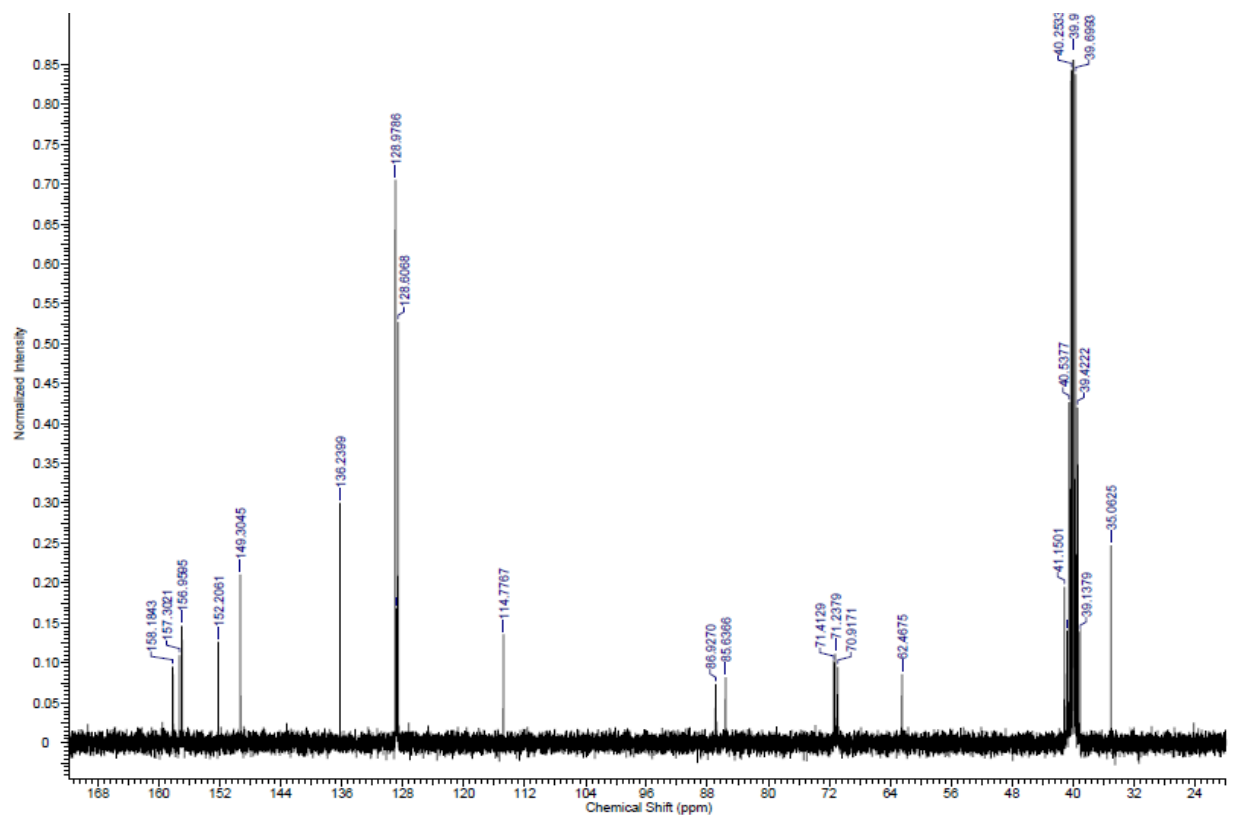


Figure S2. ¹³C NMR of S3 (top) and ¹H NMR (bottom) of compound S4.

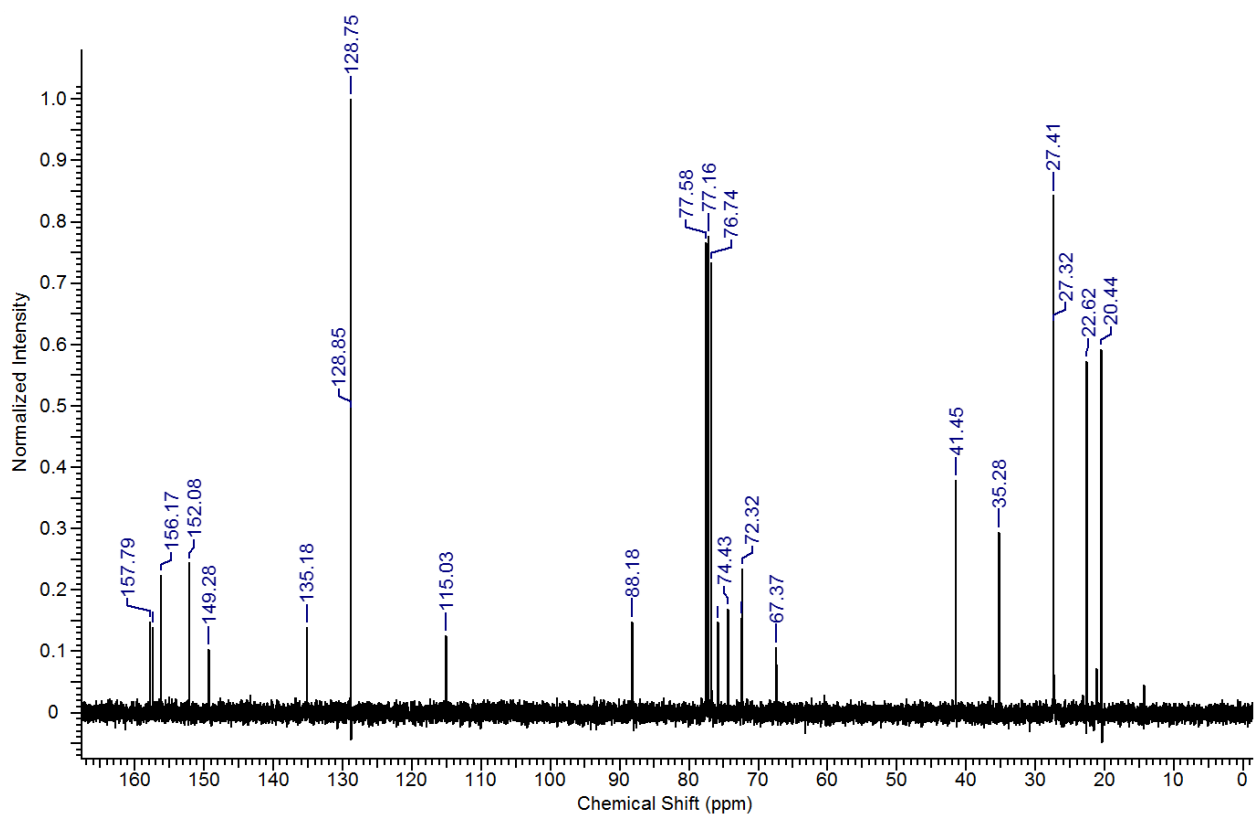
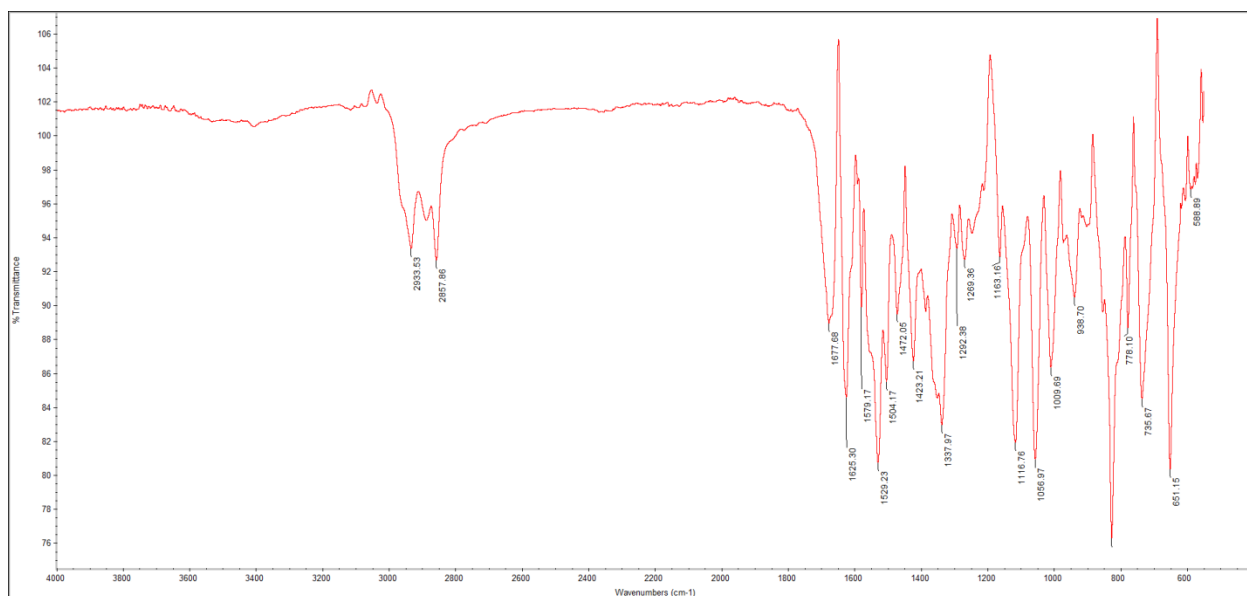


Figure S3. IR (top) and ¹³C NMR(bottom) of compound S4.

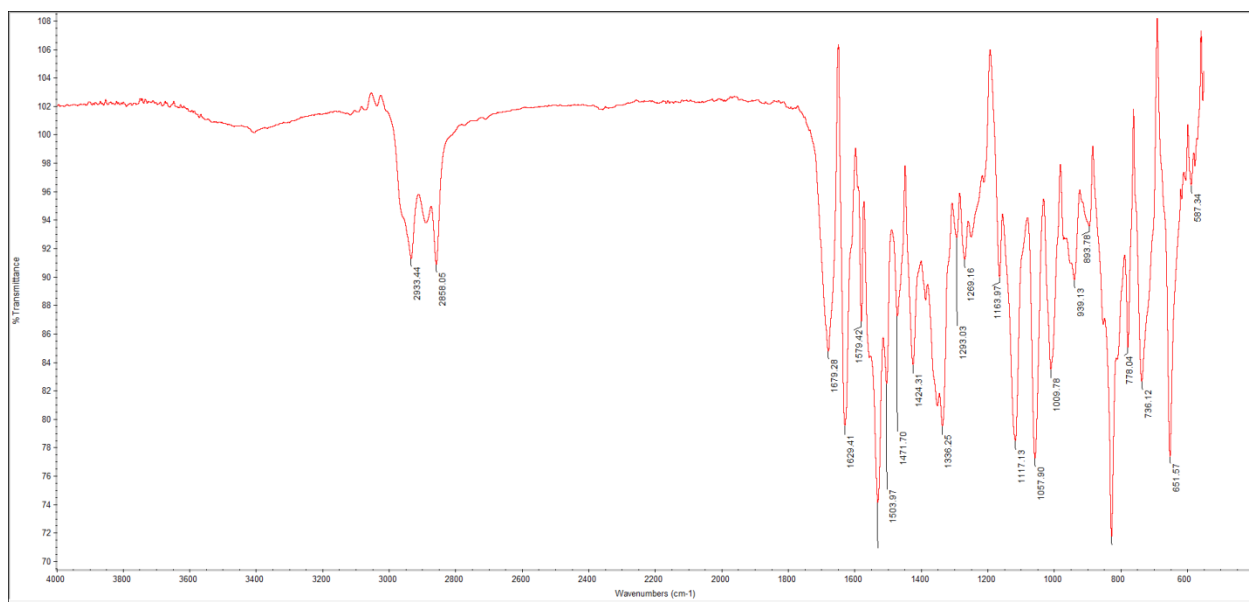
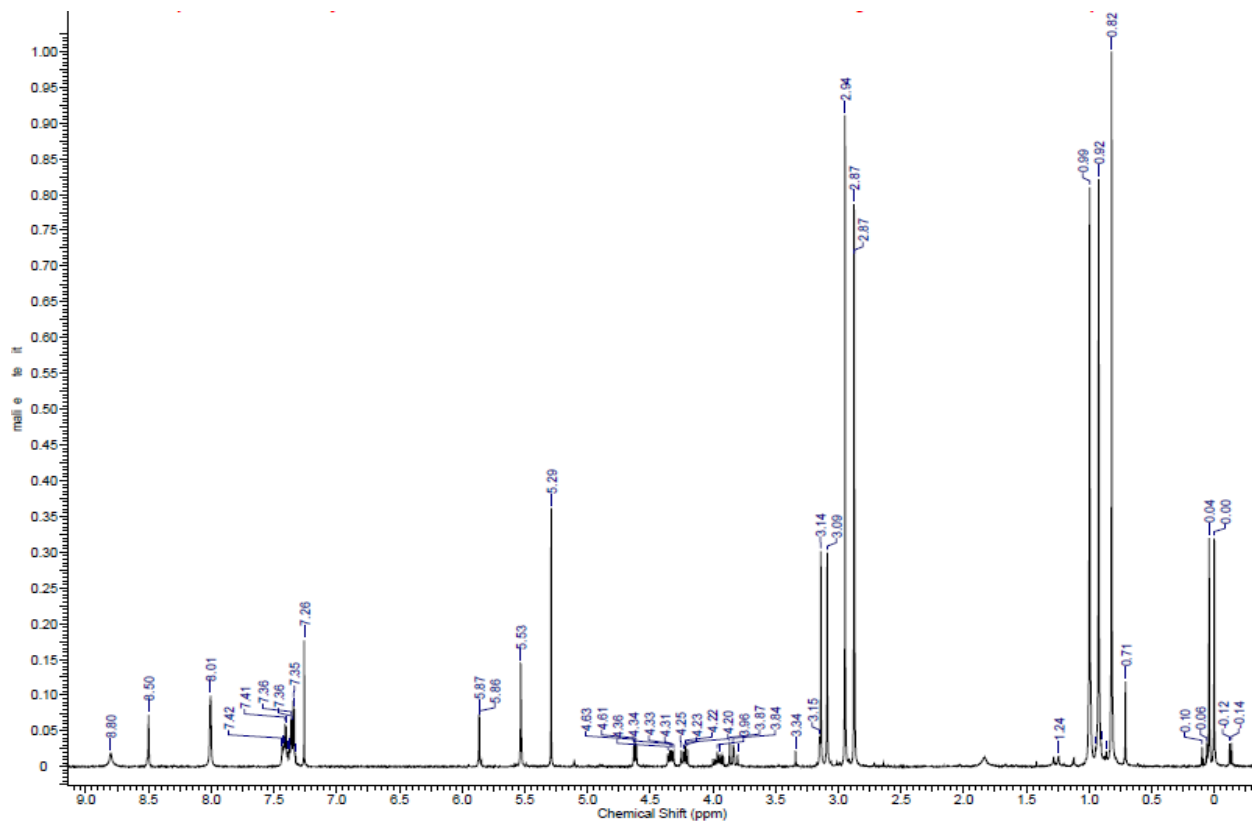


Figure S4. ¹H NMR (top) and IR of compound S5.

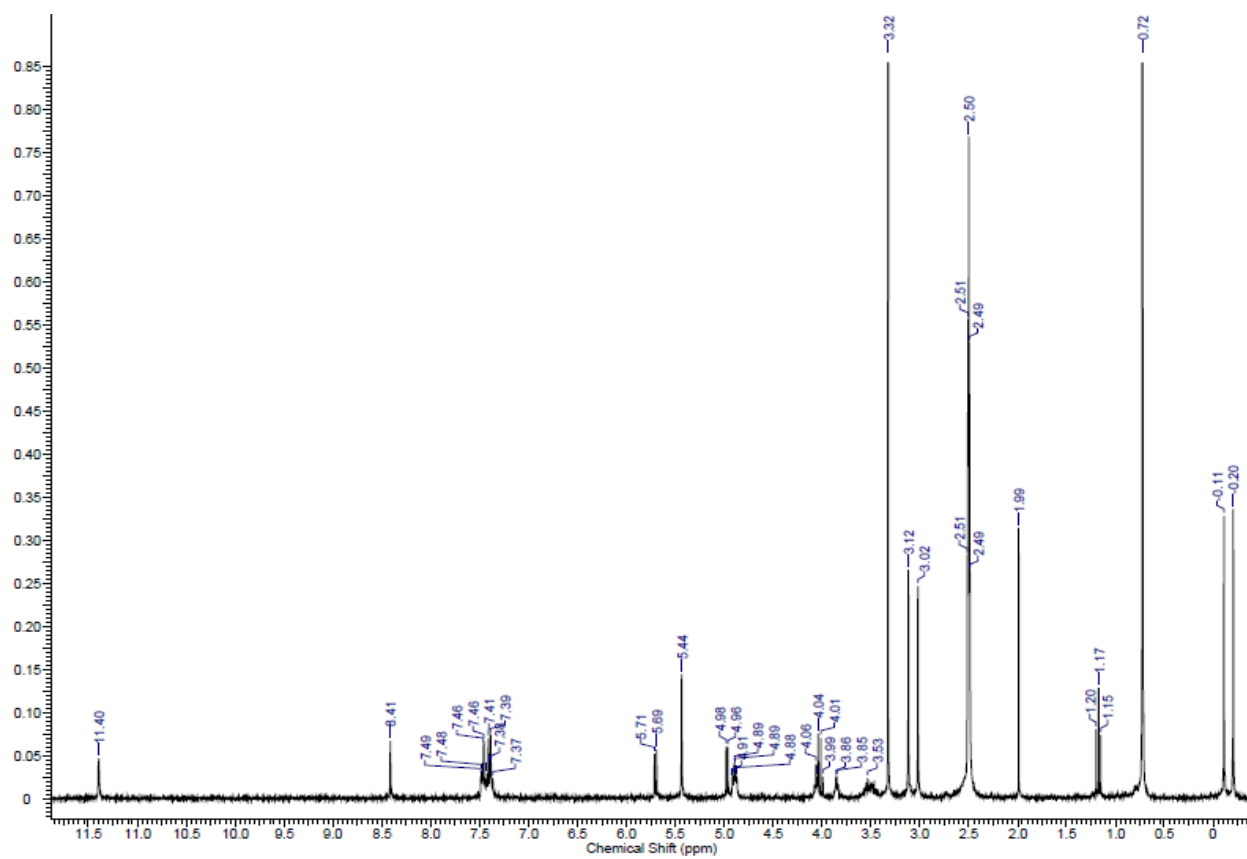
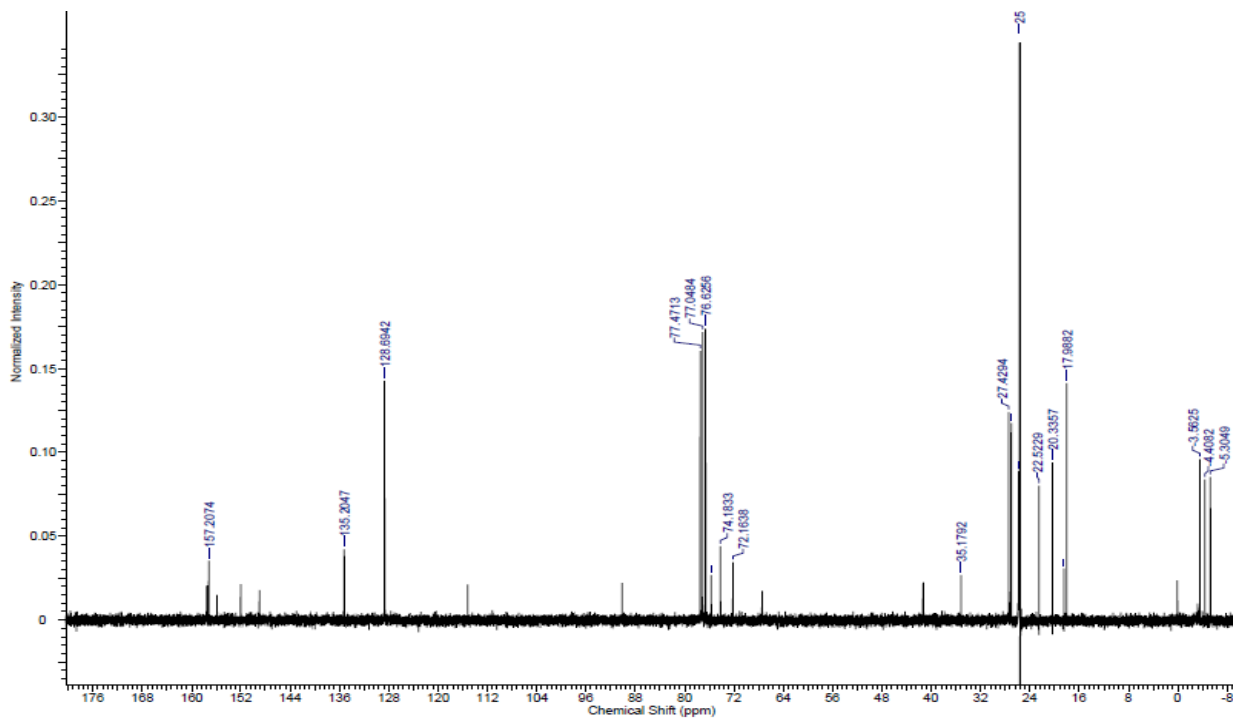


Figure S5. ¹³C NMR of S5 (top) and ¹H NMR (bottom) of compound S6.

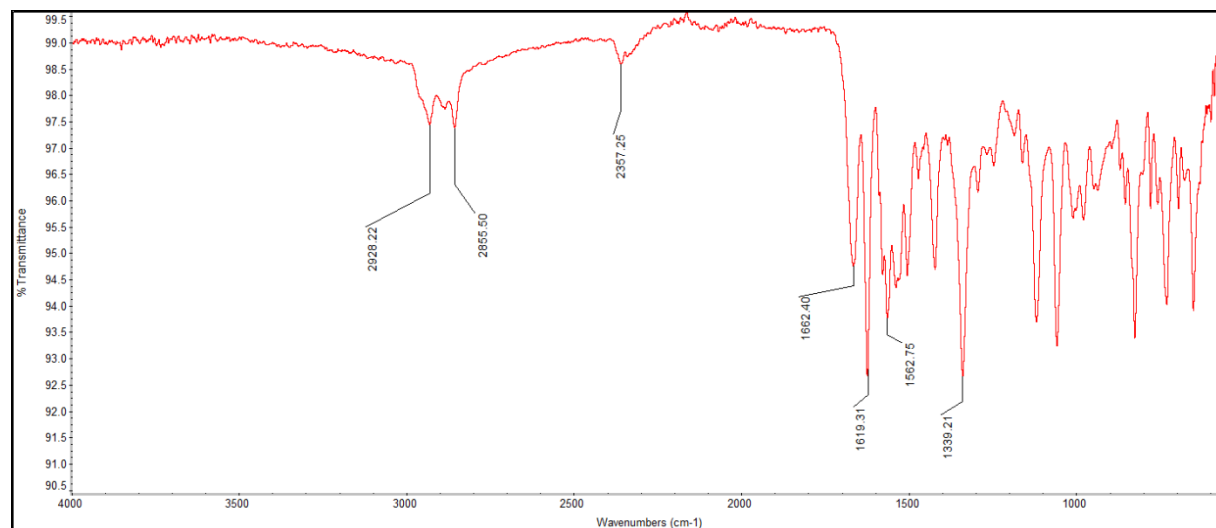
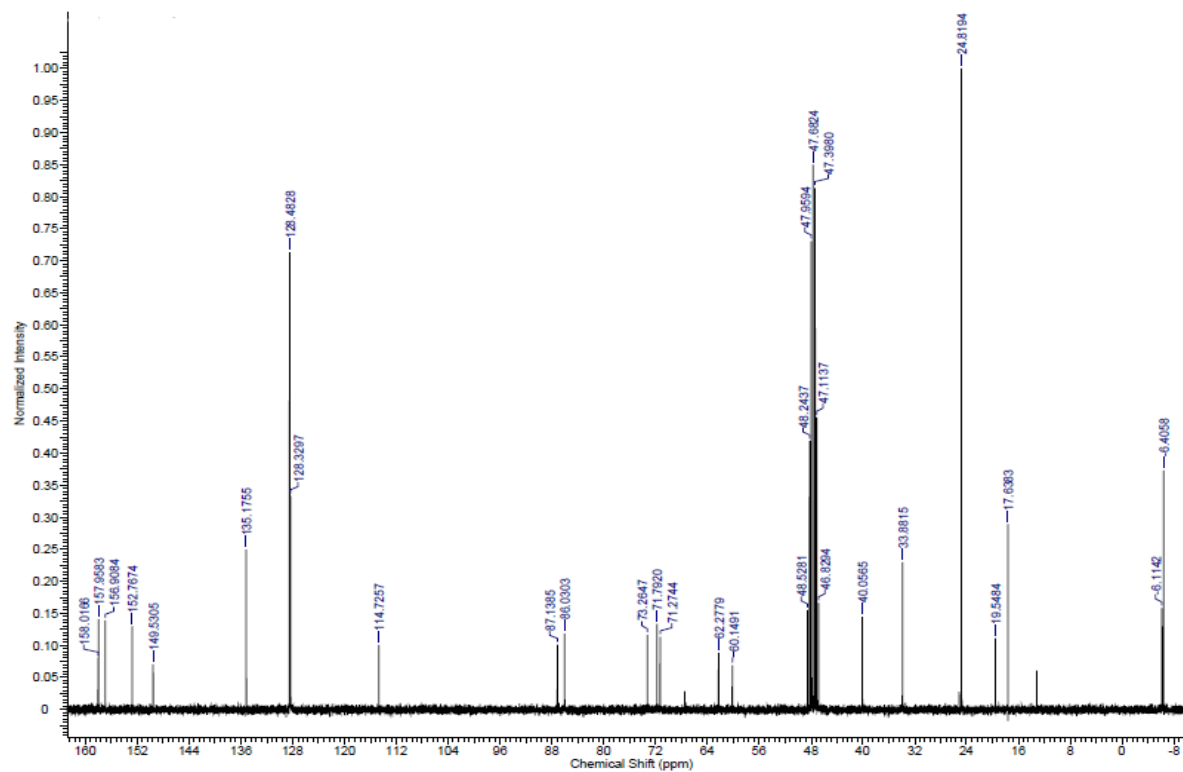


Figure S6. ¹³C NMR (top) and IR(bottom) of compound S6

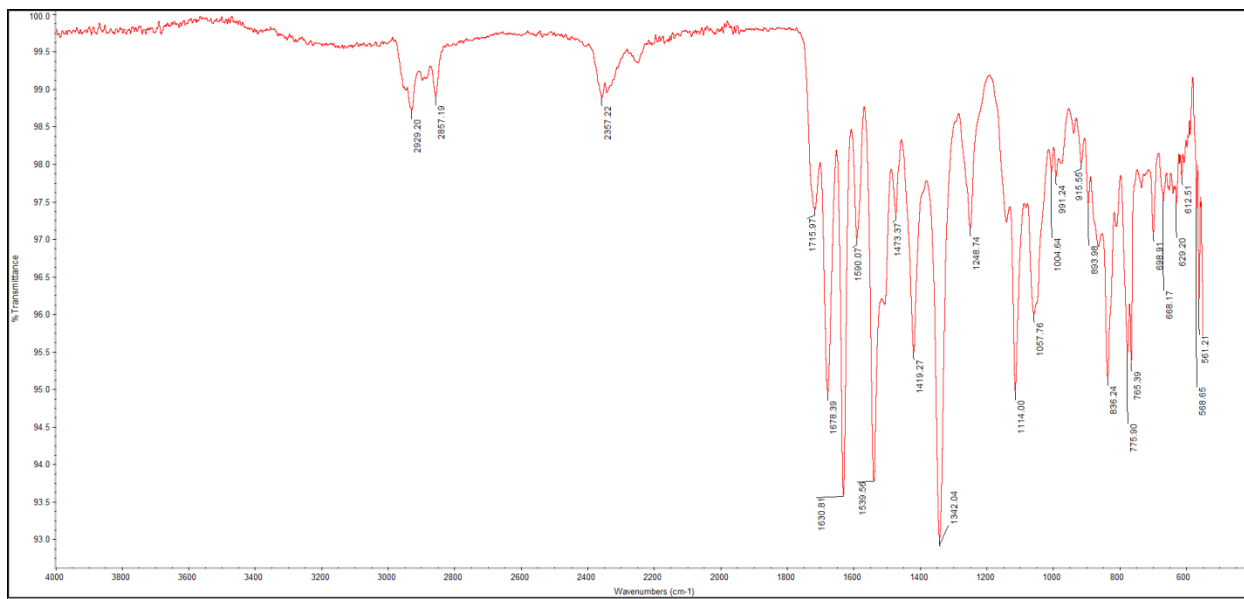
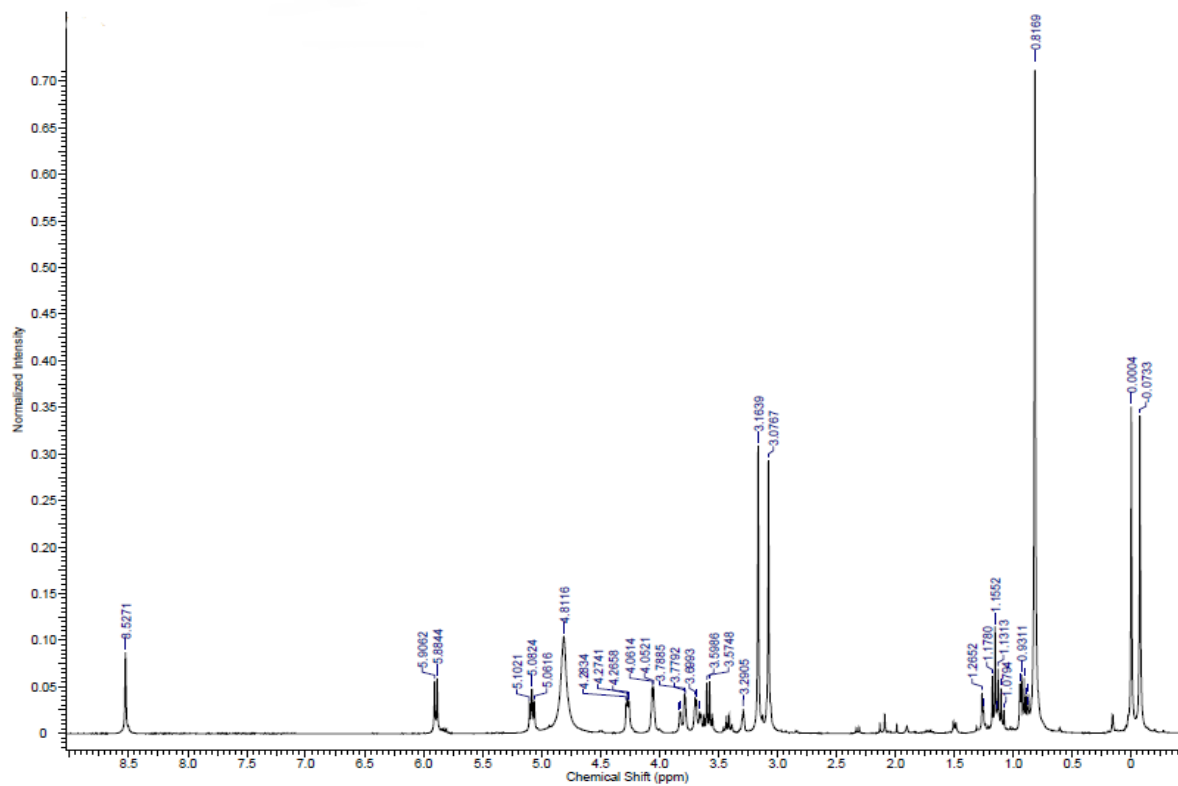


Figure S7. ¹H NMR(top) and IR(bottom) of compound S7.

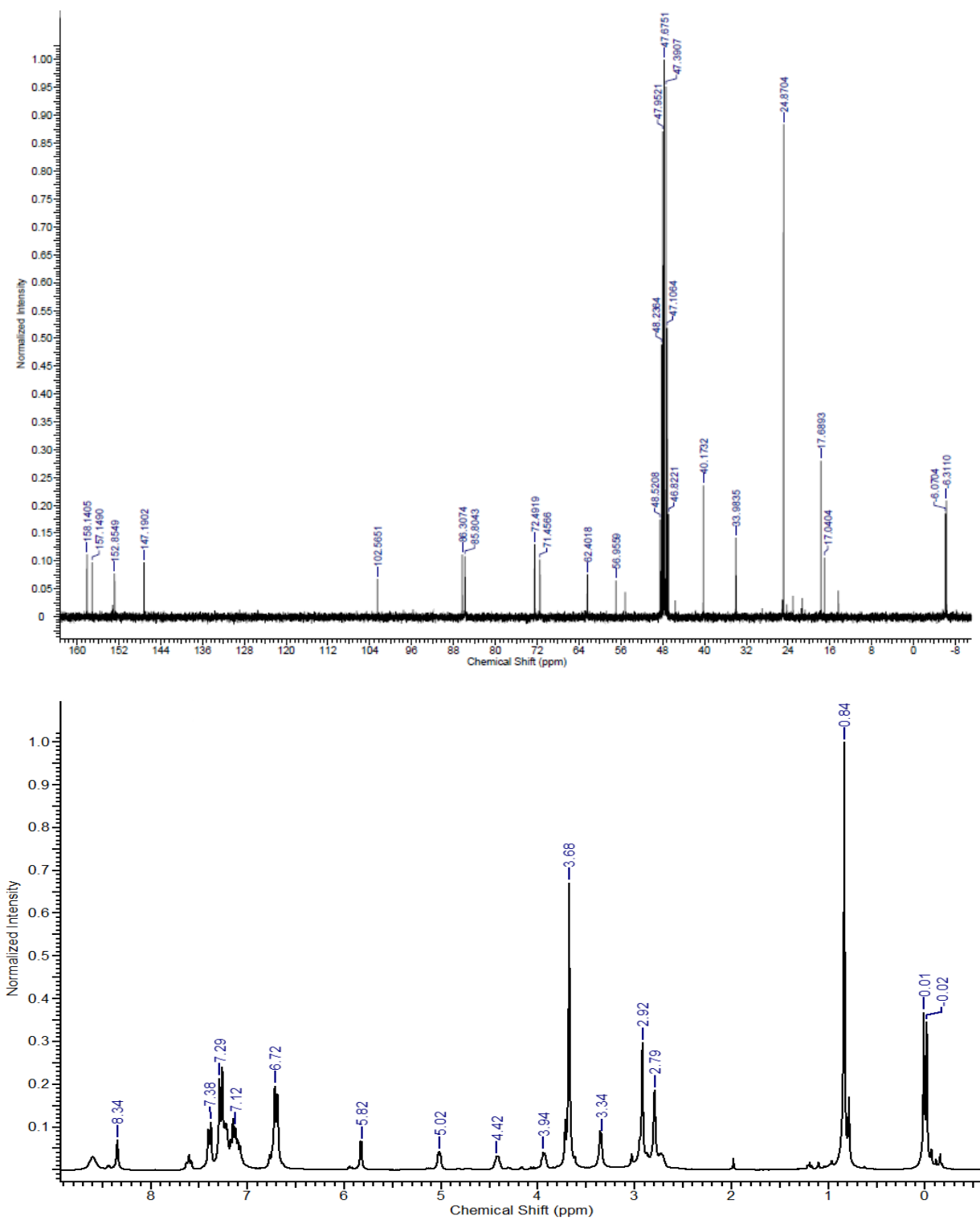


Figure S8. ^{13}C NMR (top) of S7 and ^1H NMR (bottom) of compound S8.

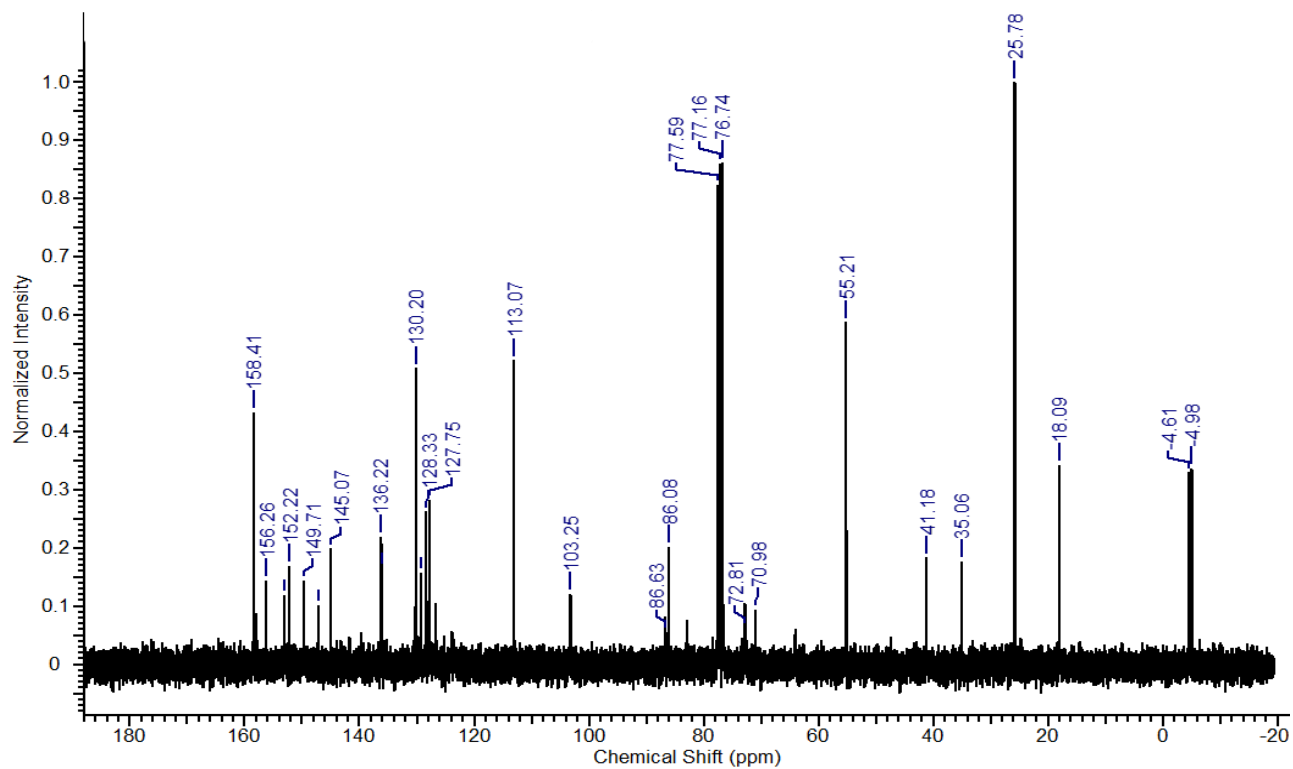
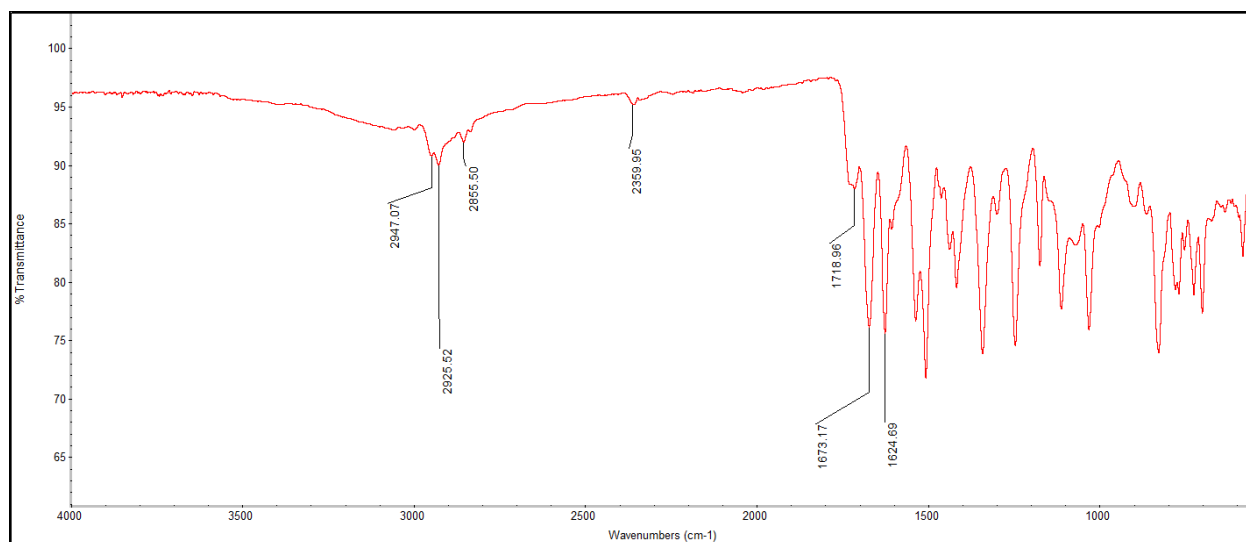


Figure S9. IR (top) and ¹³C NMR (bottom) of compound S8.

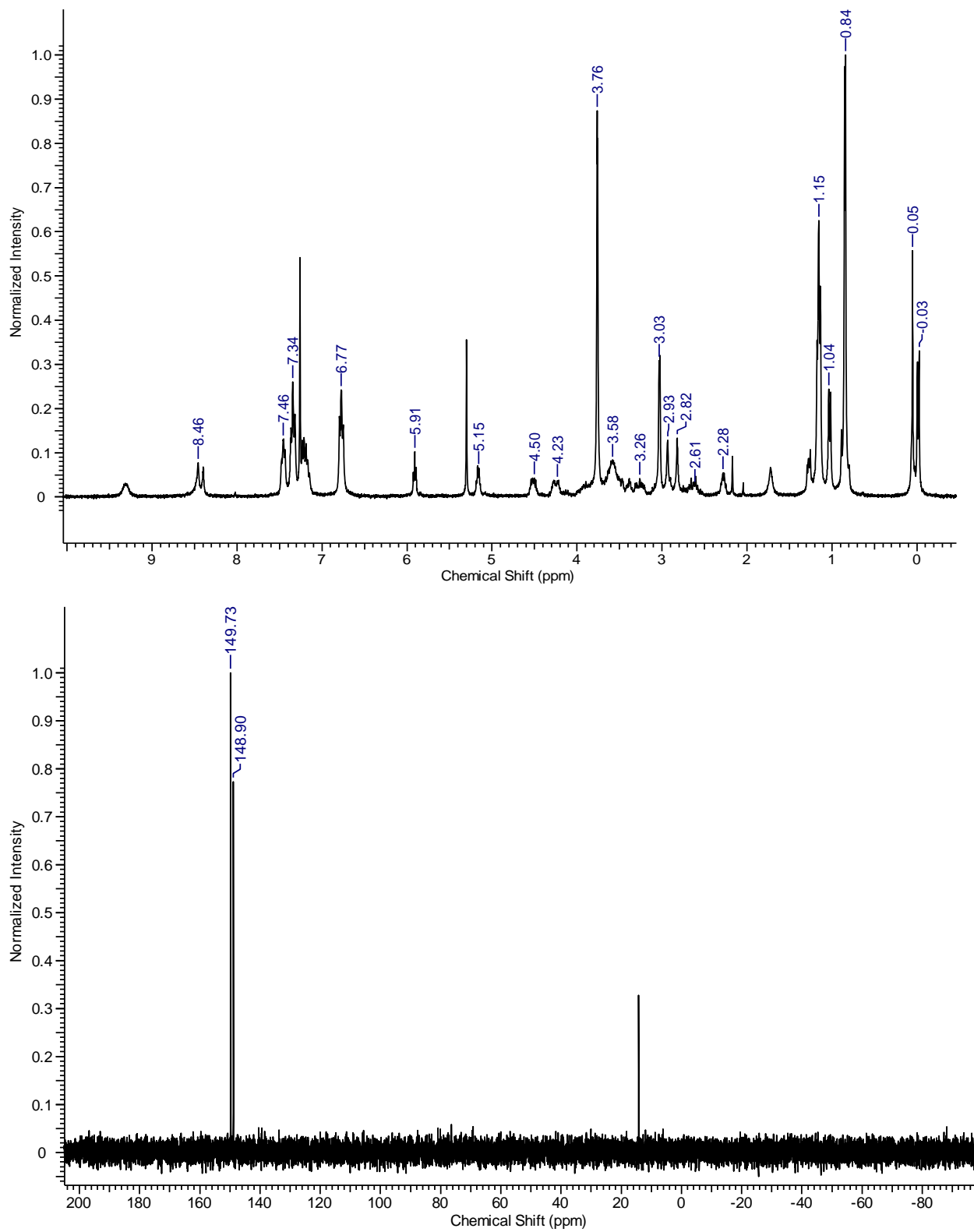


Figure S10. ^1H NMR (top) and ^{31}P NMR (bottom) of compound S9.

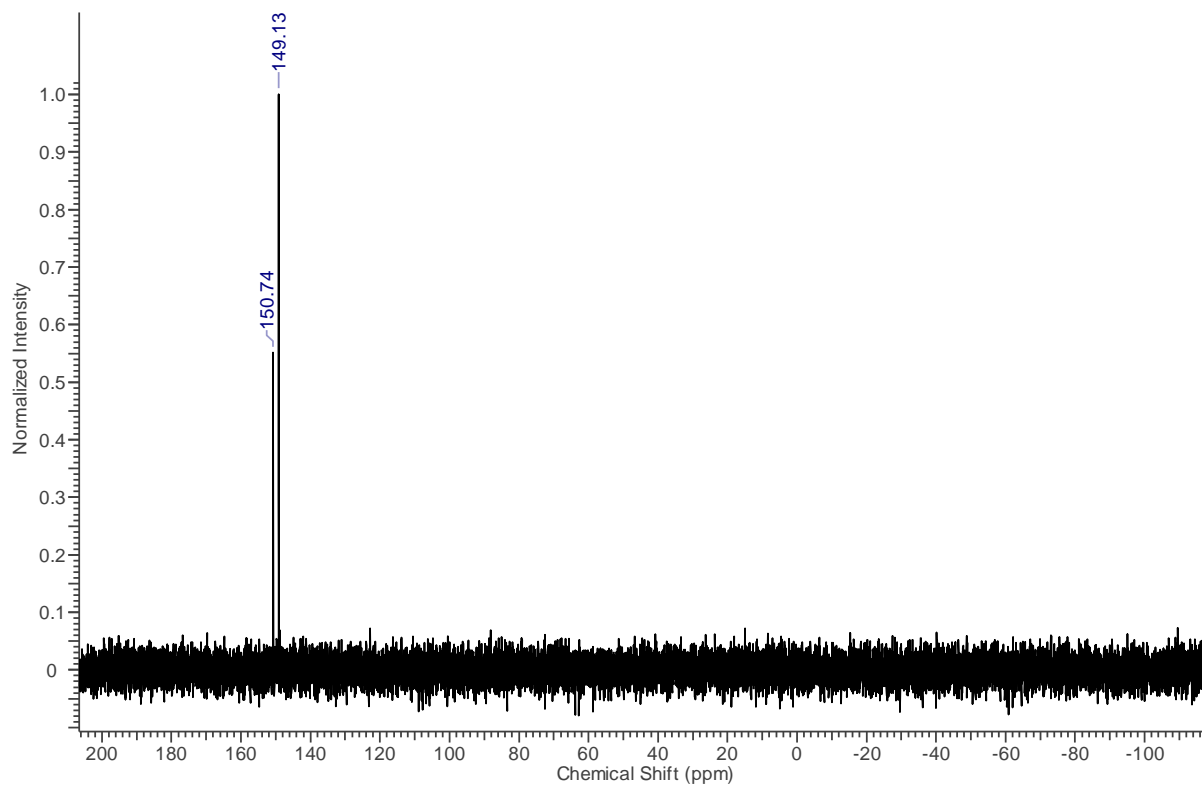
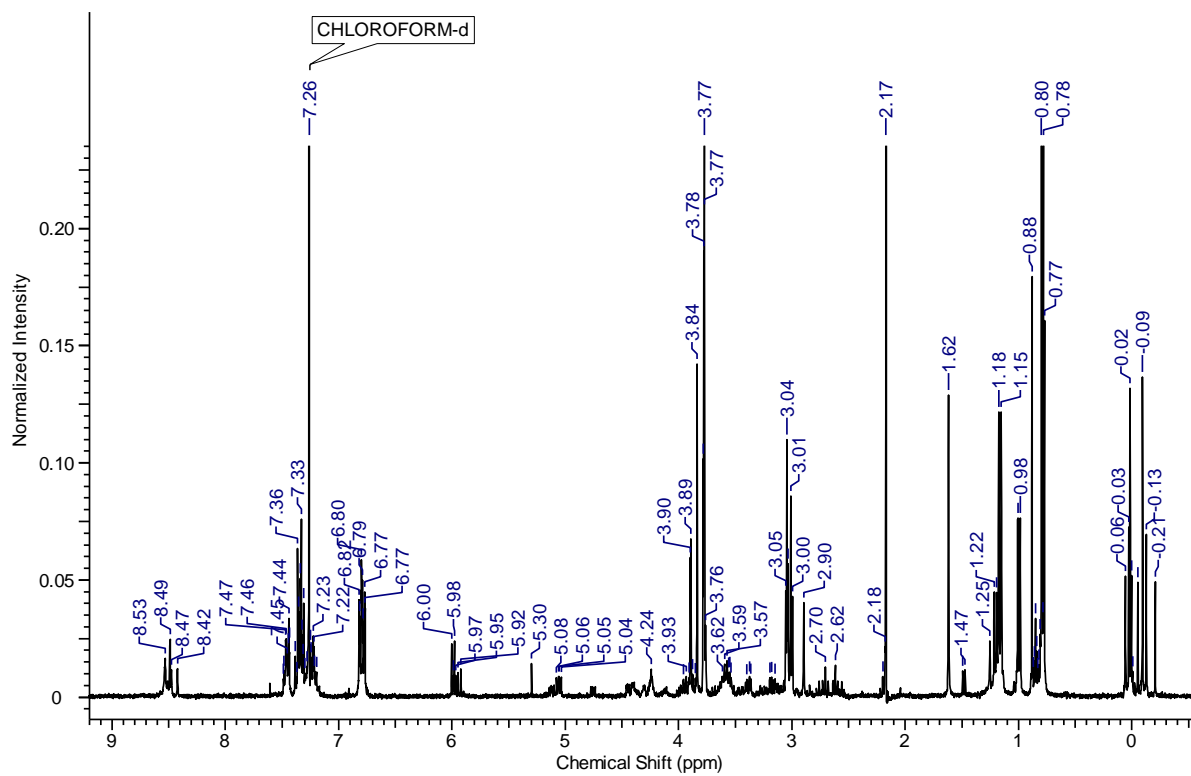


Figure S11. ^1H NMR (top) and ^{31}P NMR (bottom) of compound S10.

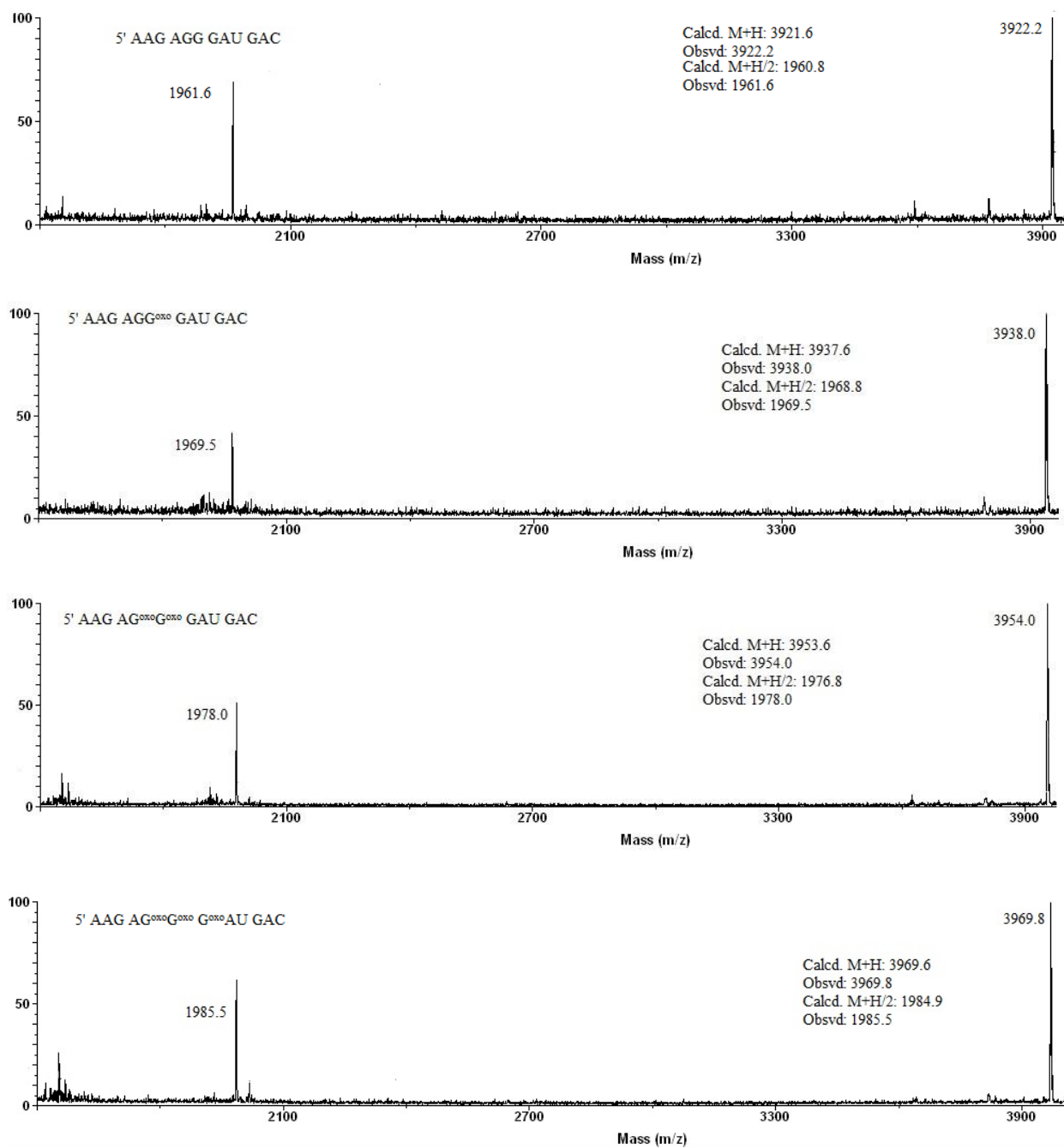


Figure S12. . MALDI-TOF MS of 1, 2, 3, and 4 (from top to bottom).

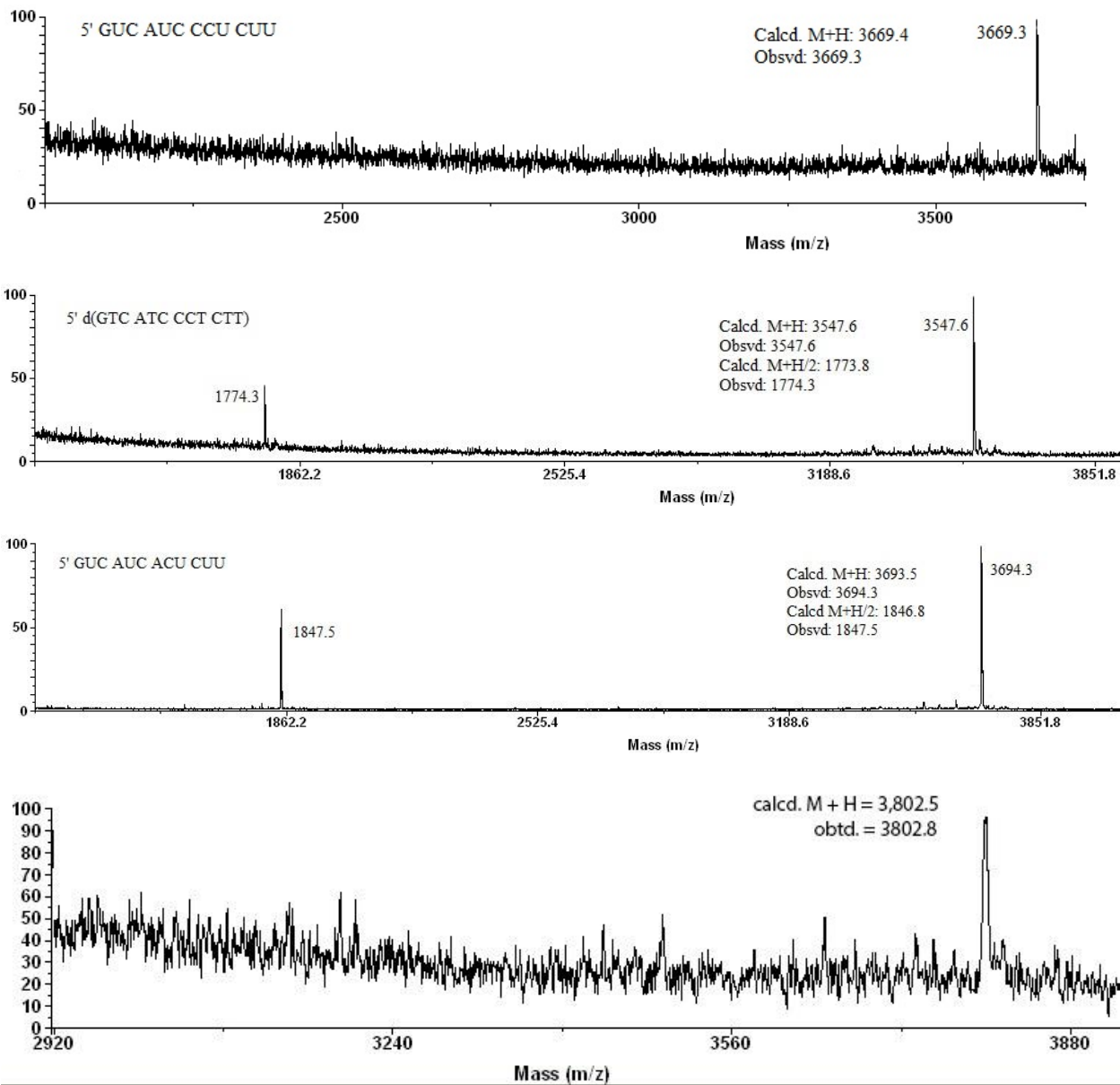


Figure S13. MALDI-TOF MS of 5, 6, 7, and 8 (from top to bottom).

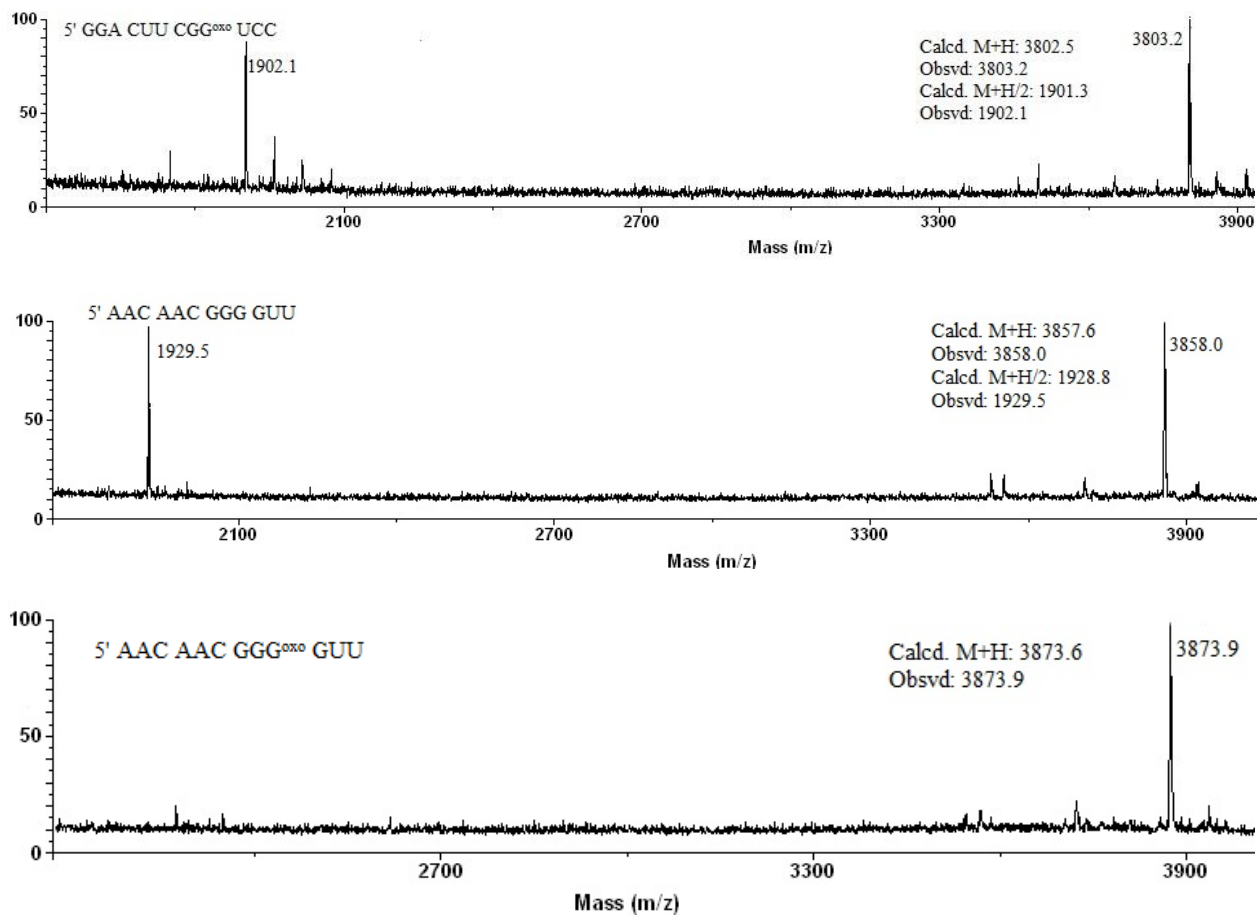


Figure S14. MALDI-TOF MS of **10**, **11**, and **12** (from top to bottom).

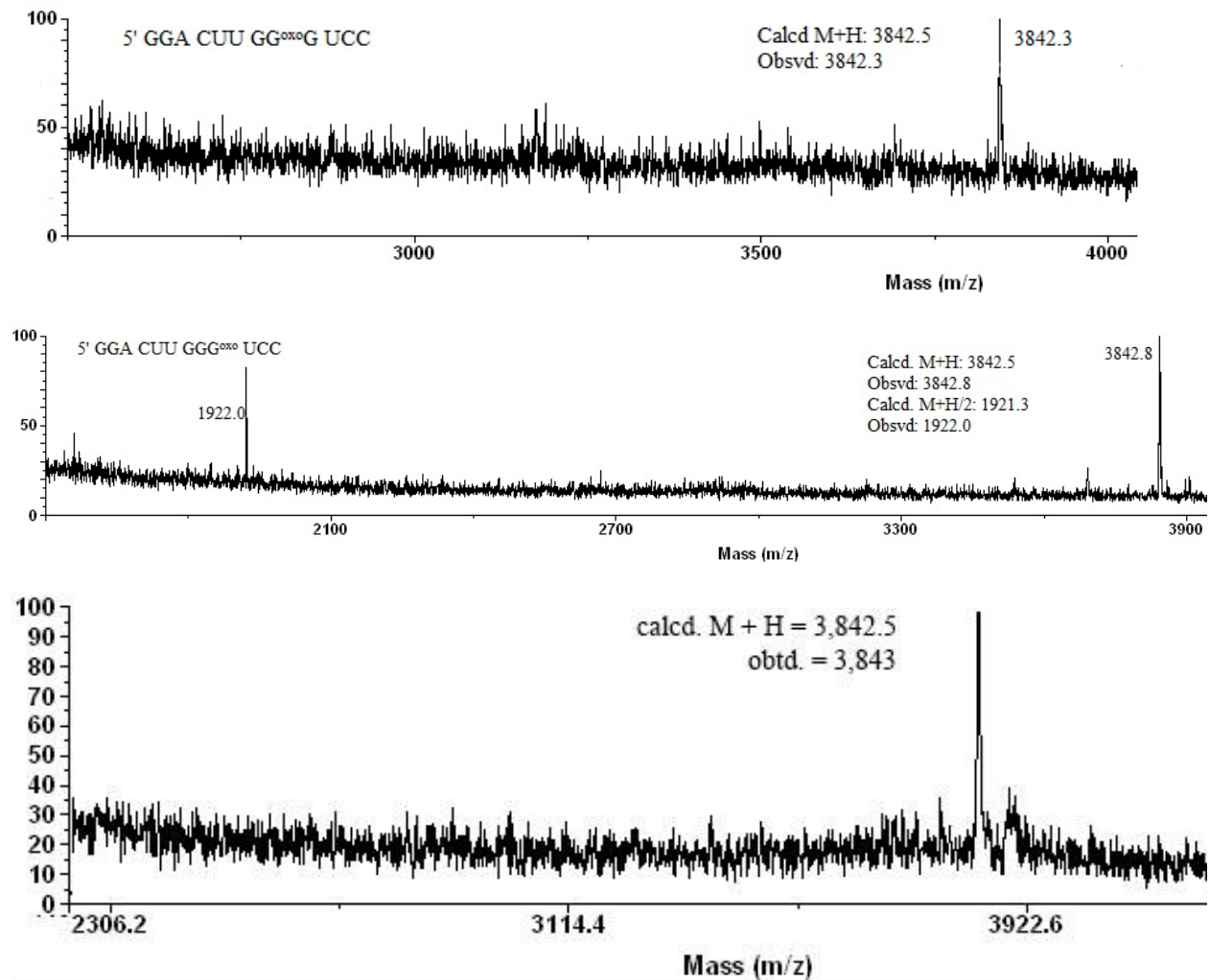


Figure S15. MALDI-TOF MS of 13, 15, and 16 (from top to bottom).

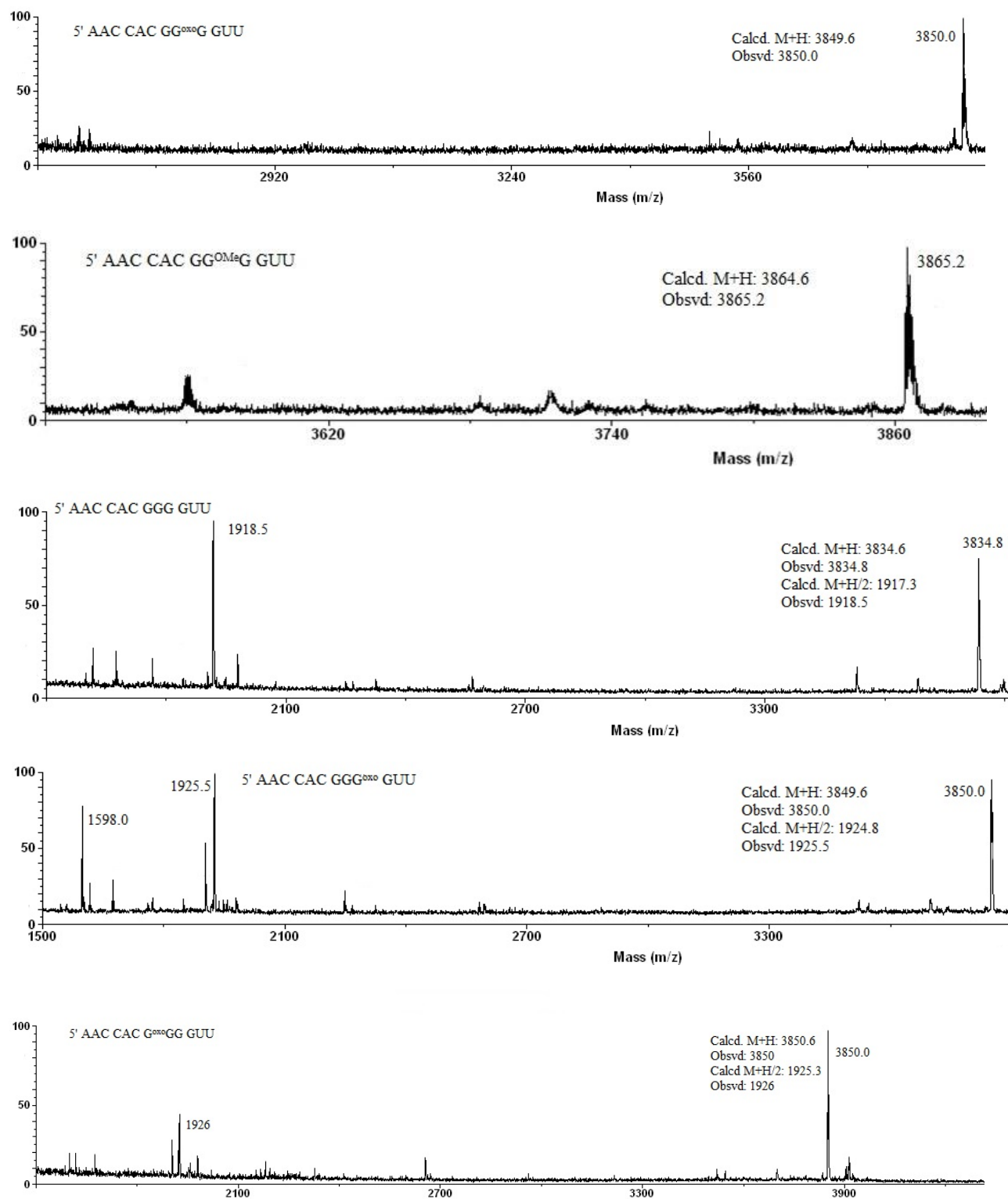


Figure S16. MALDI-TOF MS of 17, 17-OMe, 18, 19, and 20 (from top to bottom).

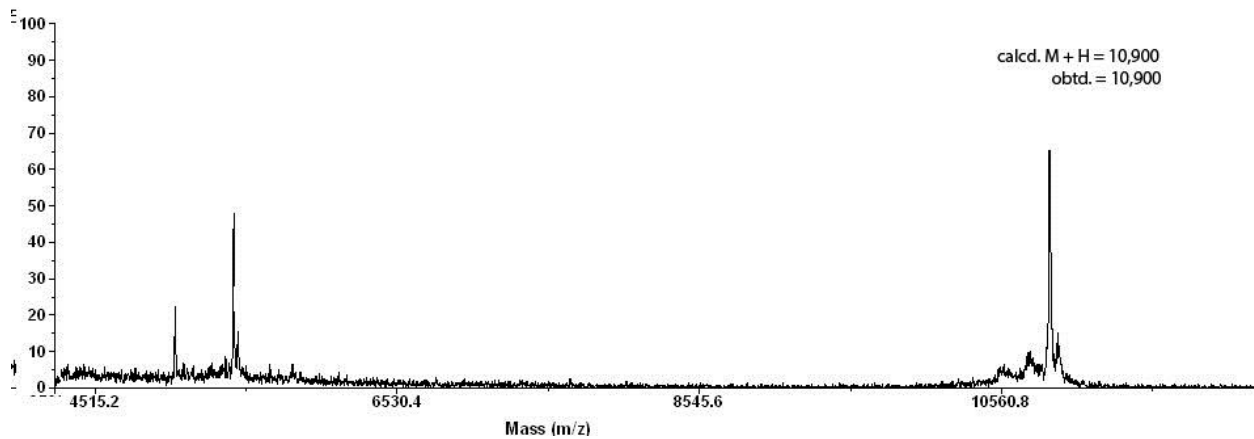
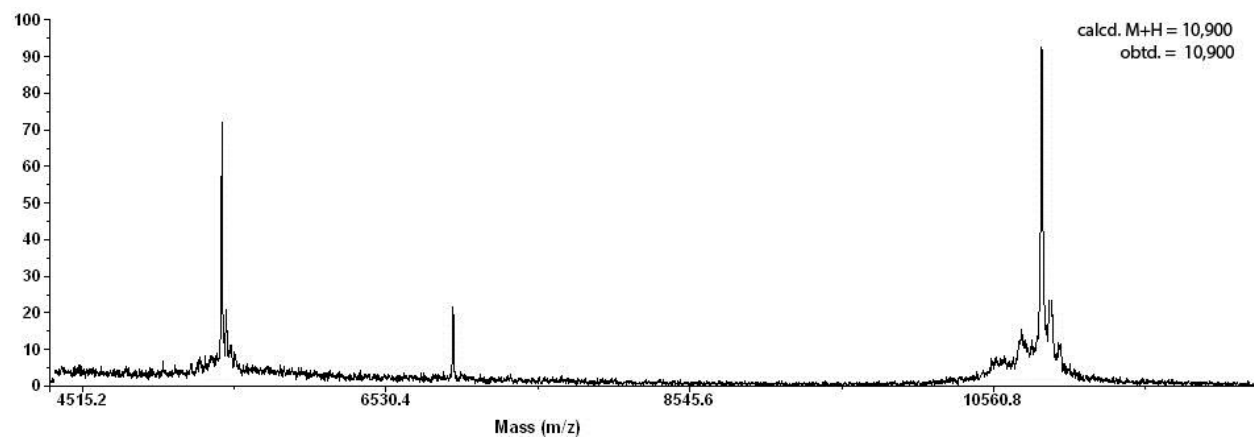
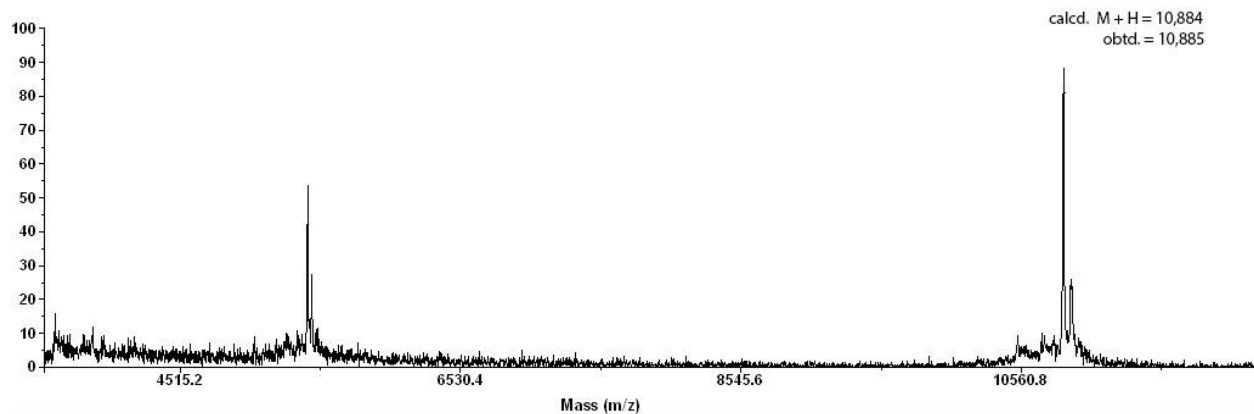


Figure S17. MALDI-TOF MS of **21**, **22**, and **23** (from top to bottom)

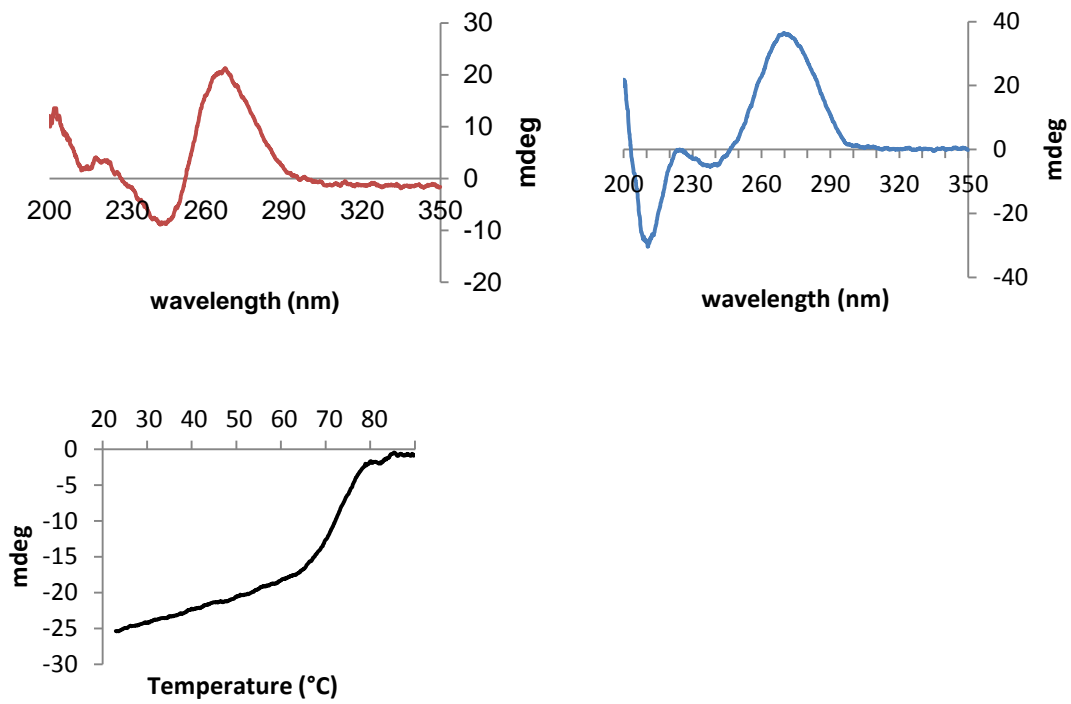


Figure S18. CDs of strands 1 (top left), 1:5 (top right), and melt of 1:5 (bottom).

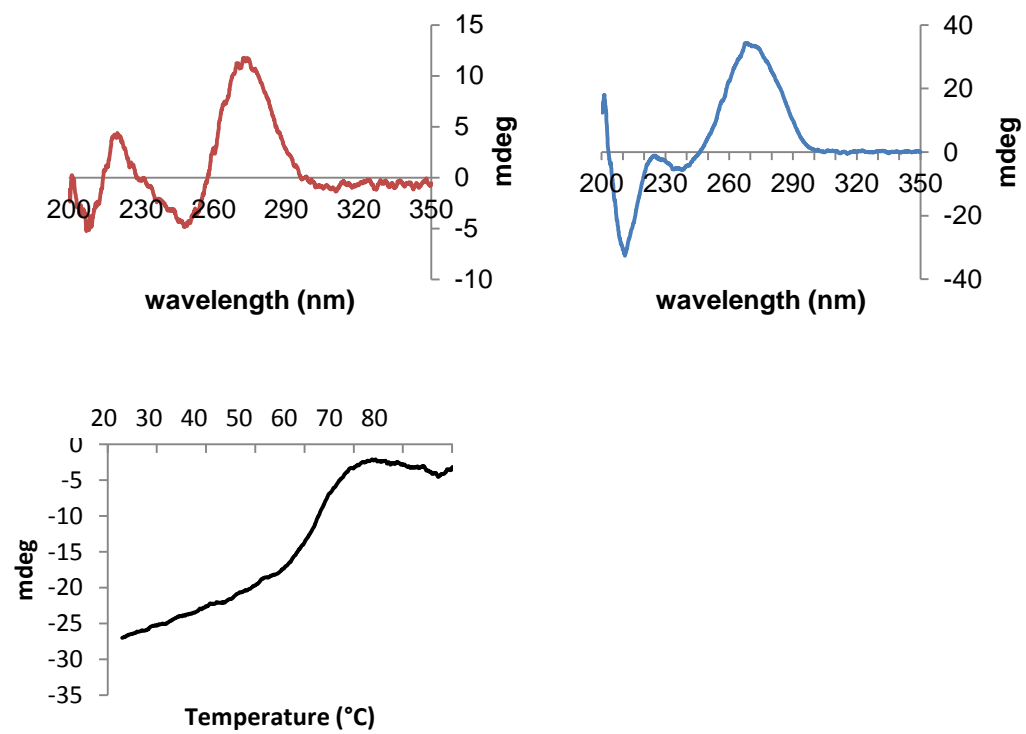


Figure S19. CDs of strand 2 (top left), 2:5 (top right), and melt of 2:5 (bottom).

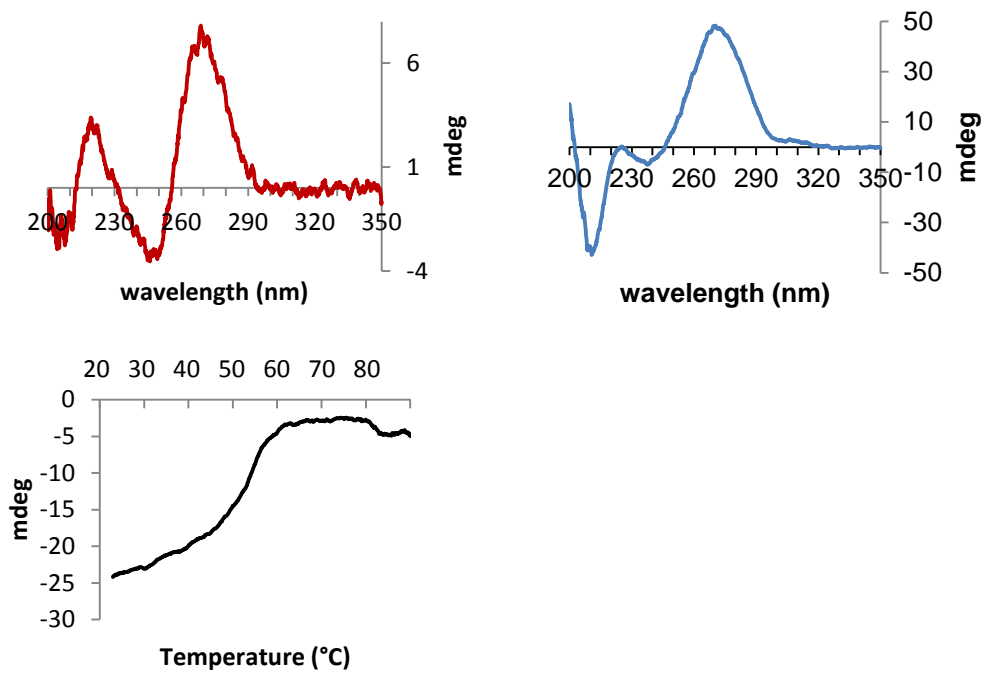


Figure S20. CDs of strand 3 (top left), 3:5 (top right), and melt of 3:5 (bottom).

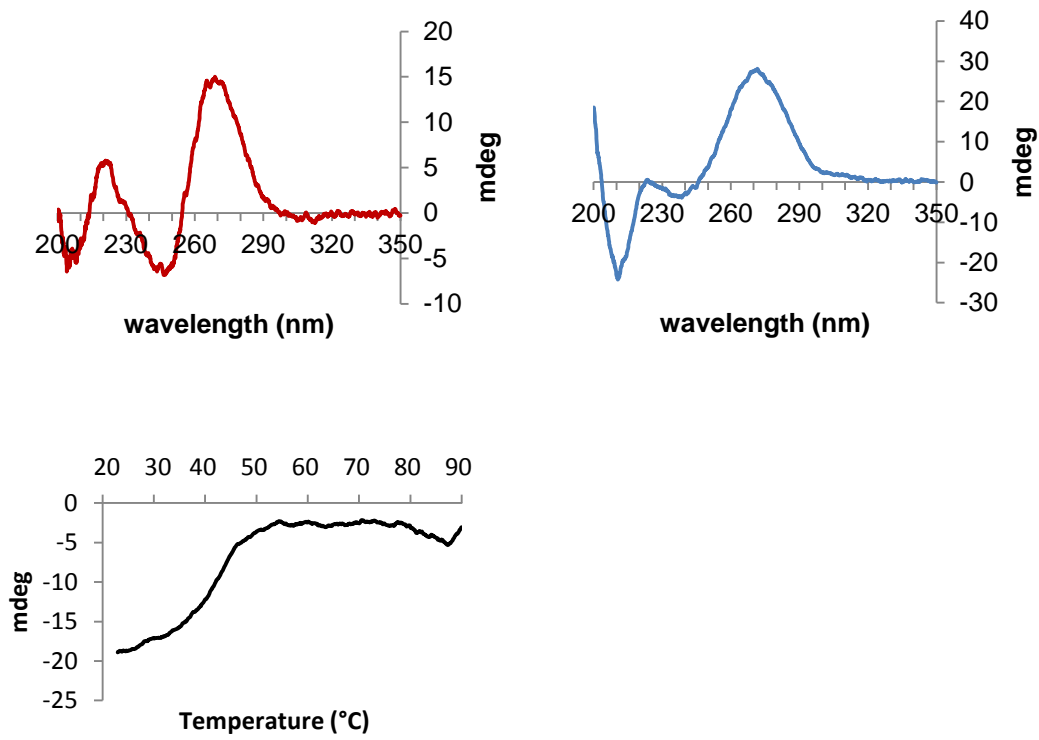


Figure S21. CDs of strand 4 (top left), 4:5 (top right), and melt of 4:5 (bottom).

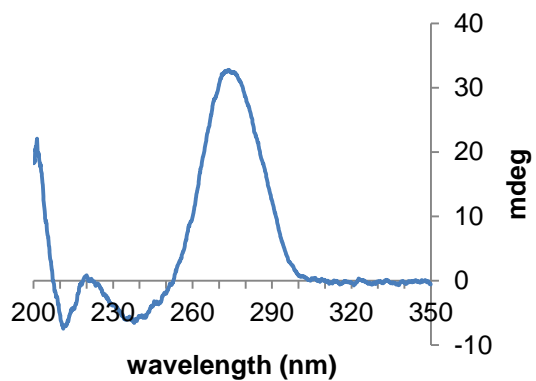


Figure S22. CD of **10**.

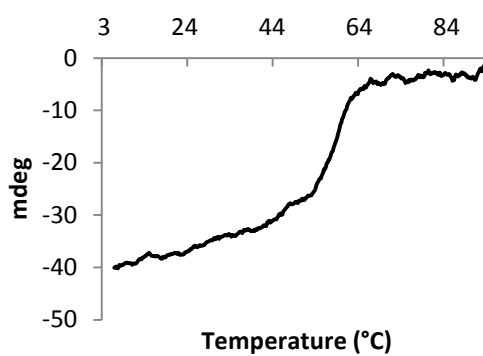
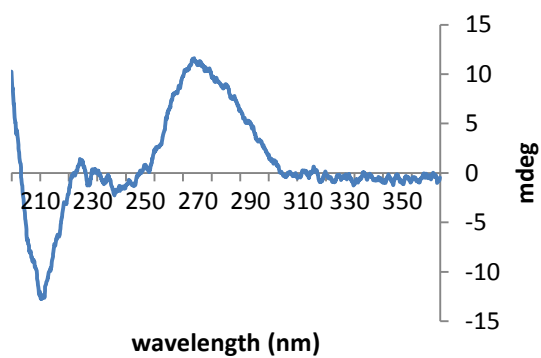


Figure S23. CD (left) and melt (right) of **1:7**.

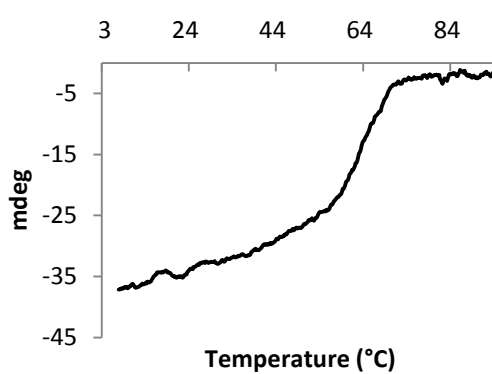
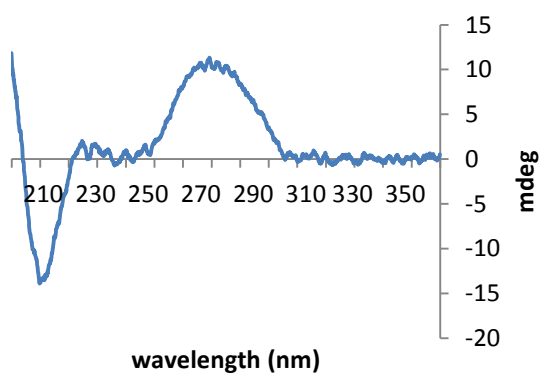


Figure S24. CD (left) and melt (right) of **2:7**.

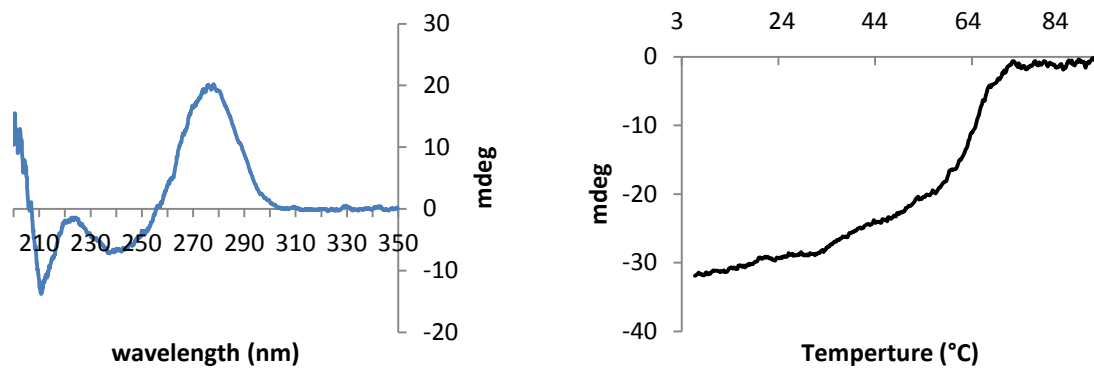


Figure S25. CD (left) and melt (right) of **1:6**.

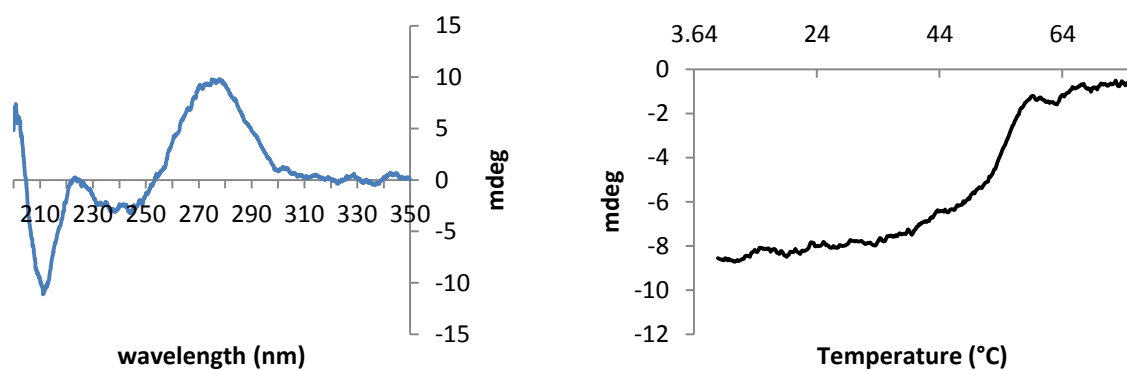


Figure S26. CD (left) and melt (right) of **2:6**.

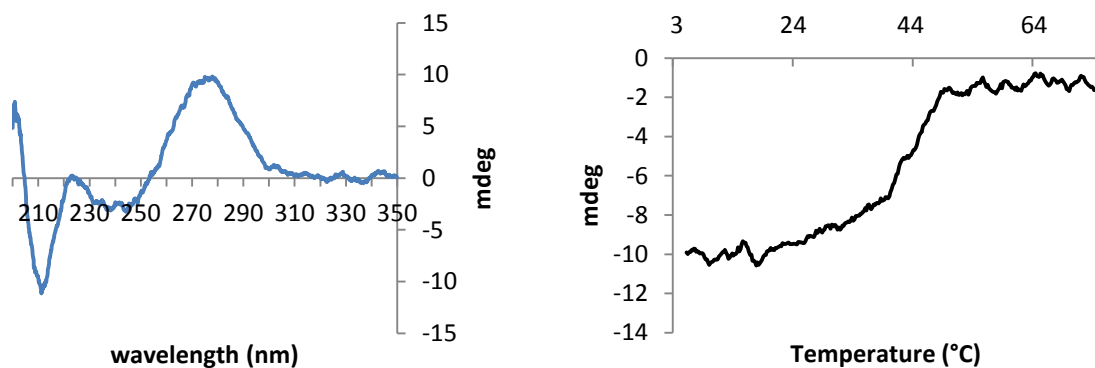


Figure S27. CD (left) and melt (right) of **3:6**.

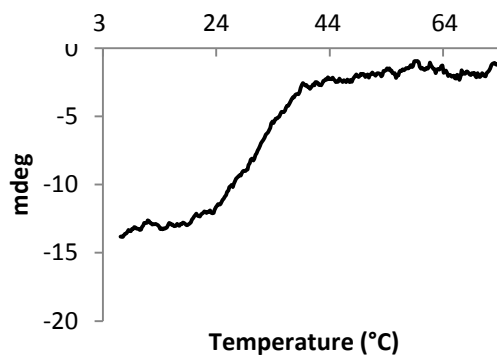
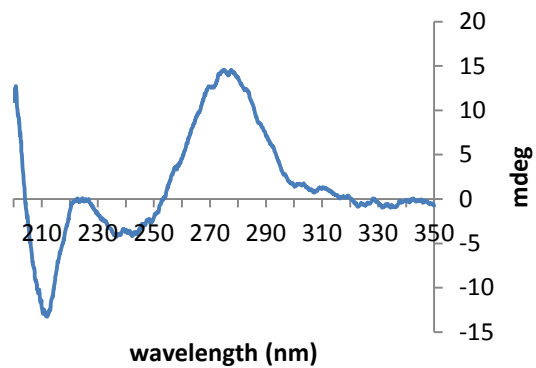


Figure S28. CD (left) and melt (right) of **4:6**.

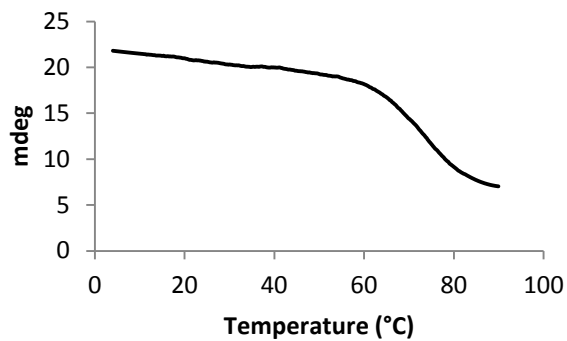
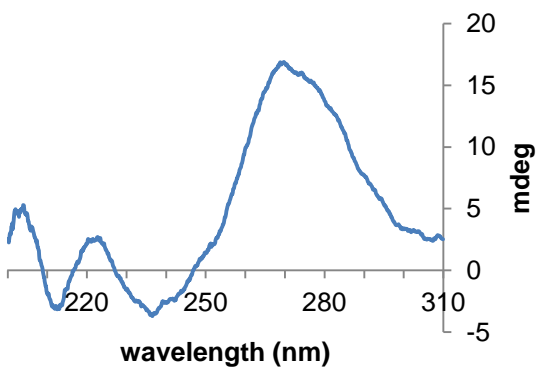


Figure S29. CD (left) and melt (right) of **8**.

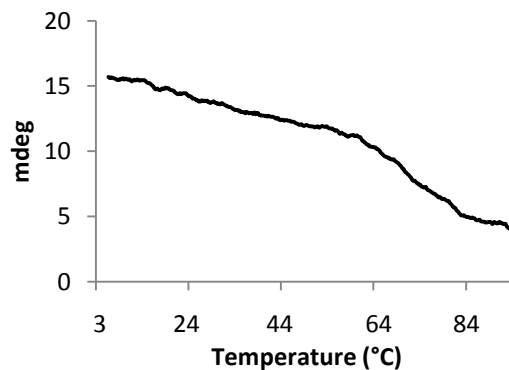
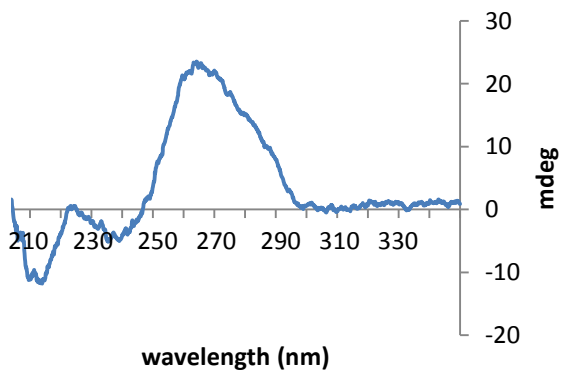


Figure S30. CD (left) and melt (right) of **9**.

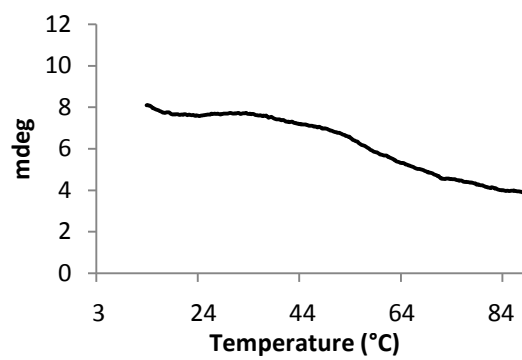
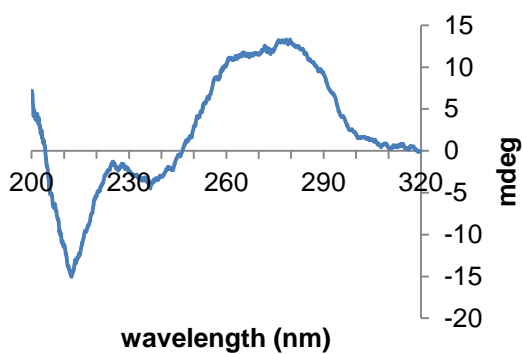


Figure S31. CD (left) and melt (right) of **10**.

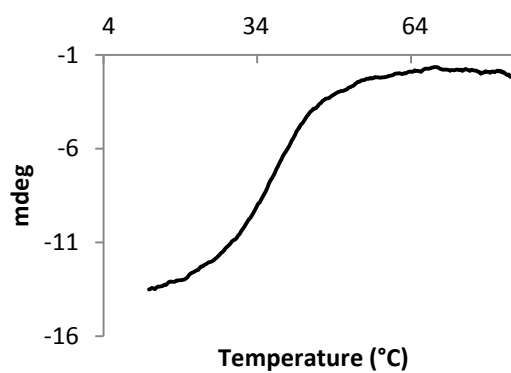
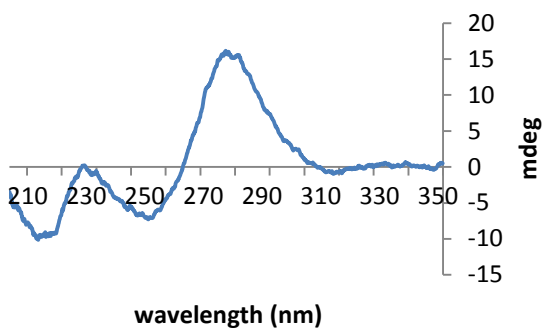


Figure S32. CD (left) and melt (right) of **11**.

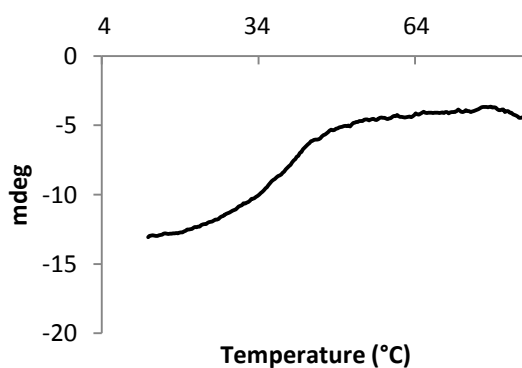
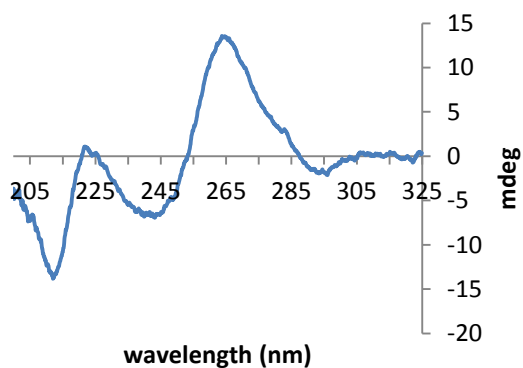


Figure S33. CD (left) and melt (right) of **12**.

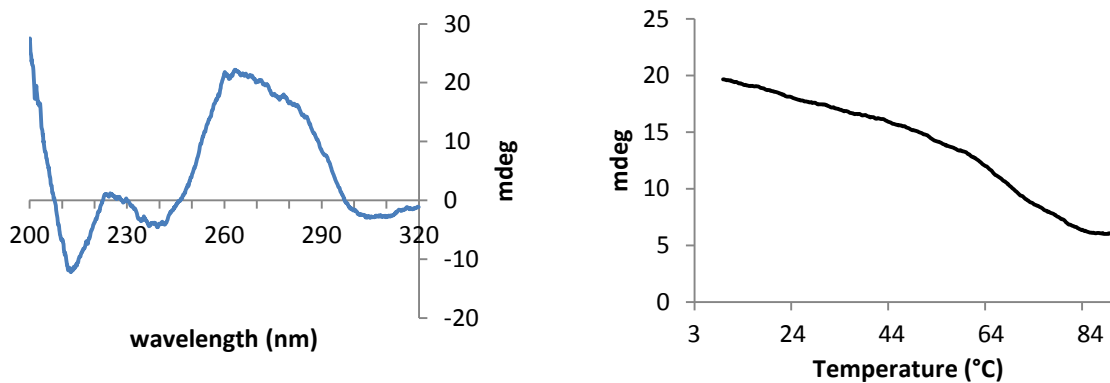


Figure S34. CD (left) and melt (right) of **13**.

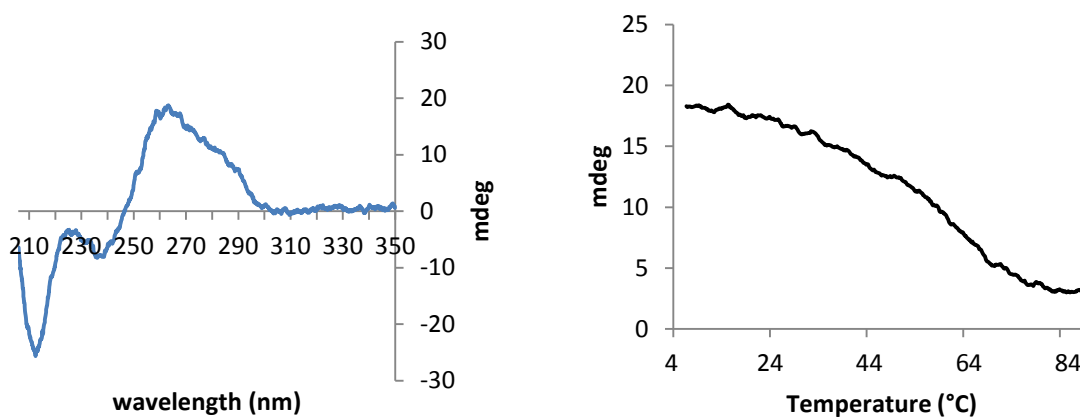


Figure S35. CD (left) and melt (right) of **14**.

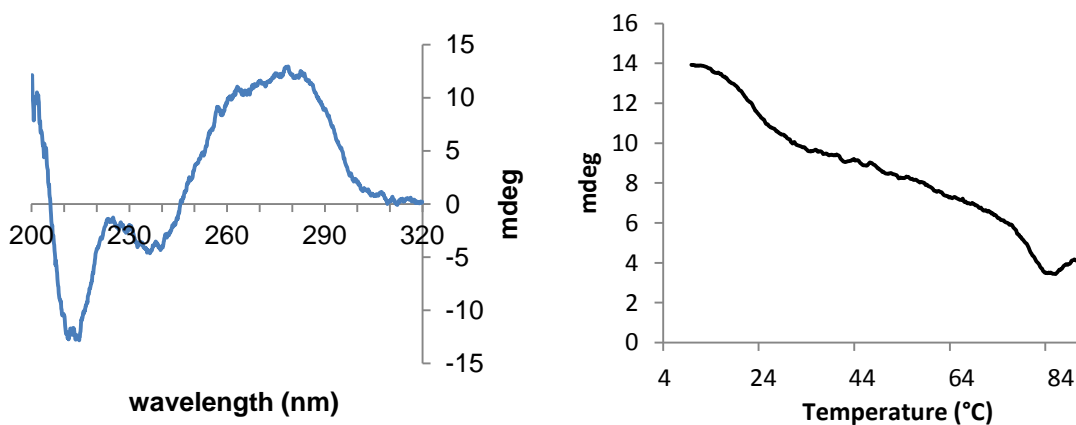


Figure S36. CD (left) and melt (right) of **15**.

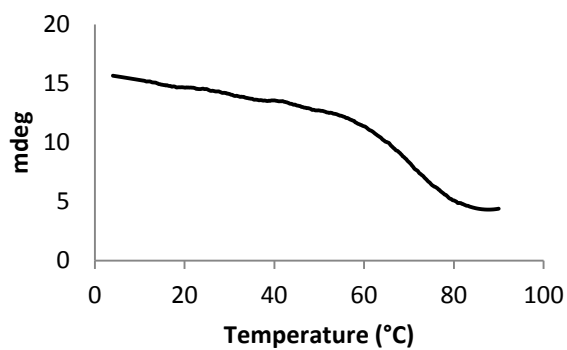
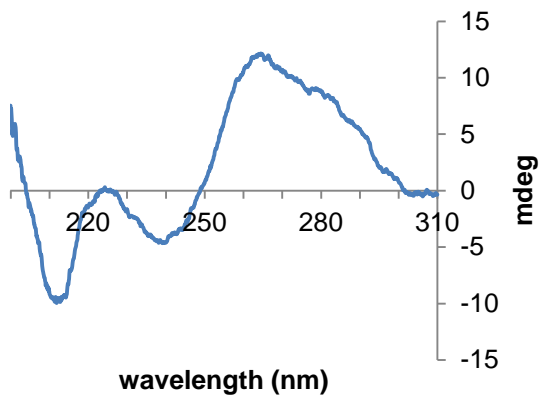


Figure S37. CD (left) and melt (right) of **16**.

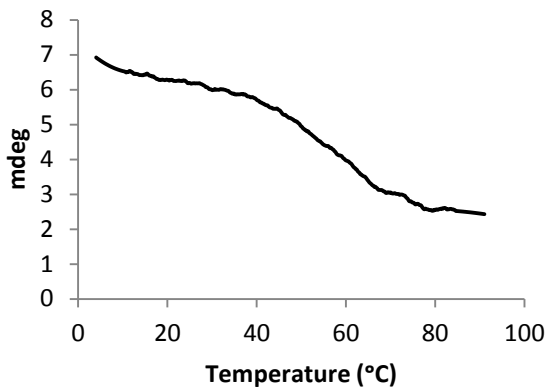
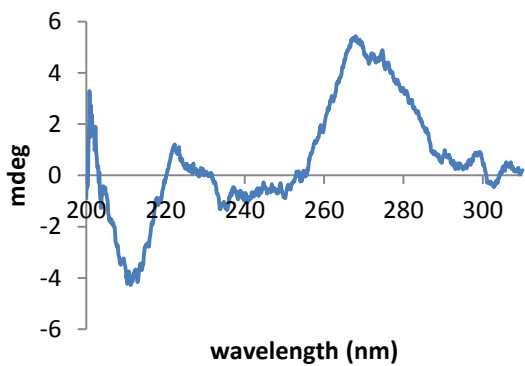


Figure S38. CD (left) and melt (right) of **17'**.

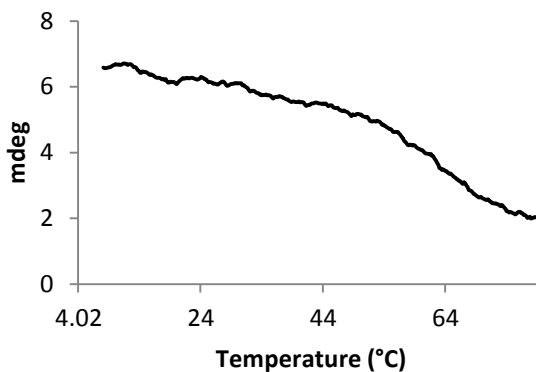
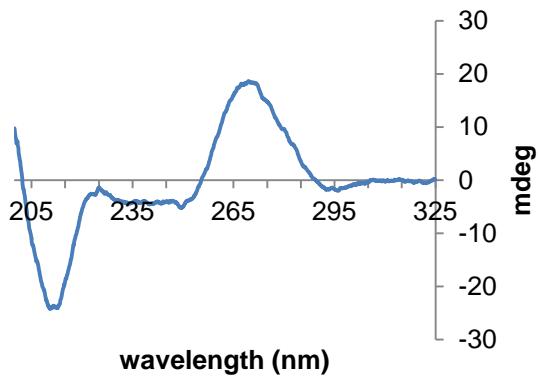


Figure S39. CD (left) and melt (right) of **17**.

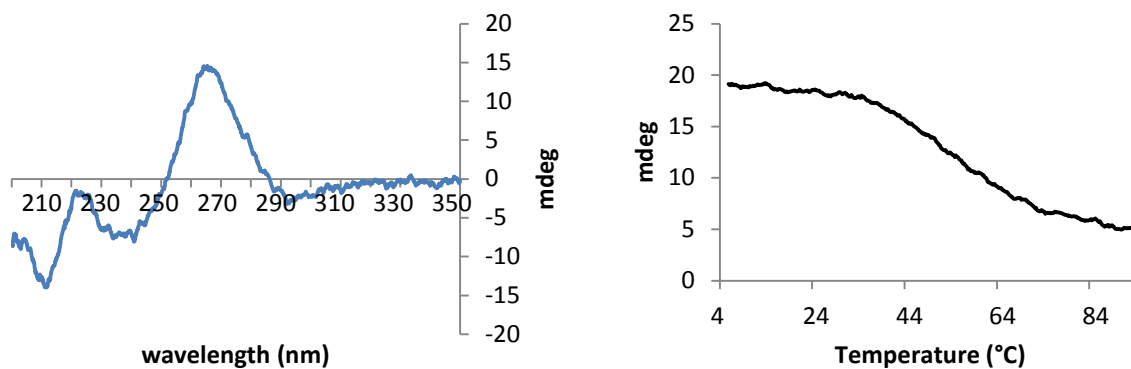


Figure S40. CD (left) and melt (right) of **17-OMe**.

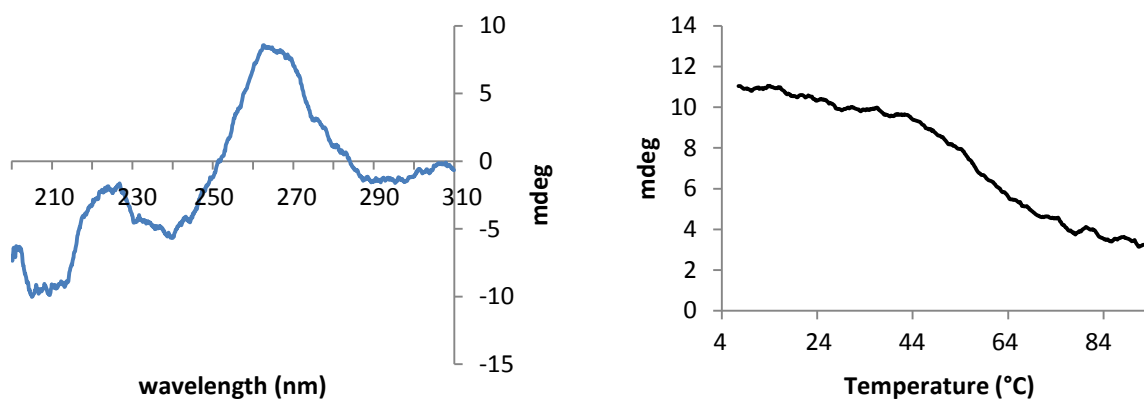


Figure S41. CD (left) and melt (right) of **18**.

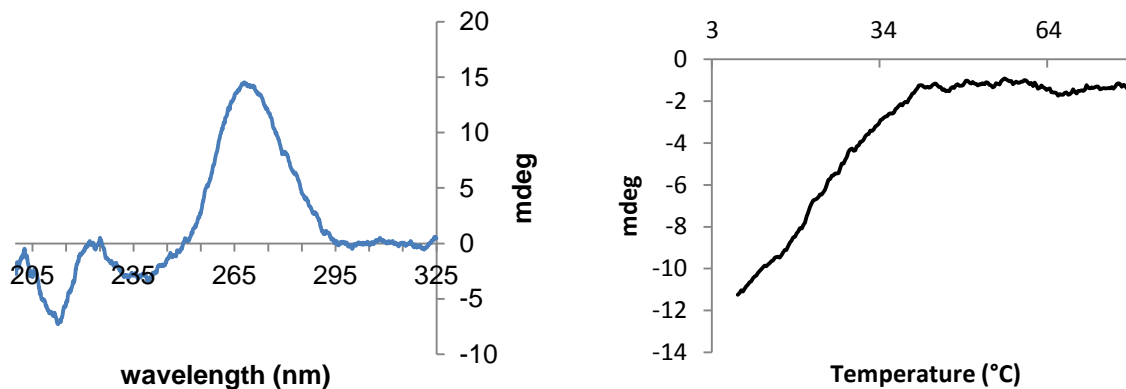


Figure S42. CD (left) and melt (right) of **19**.

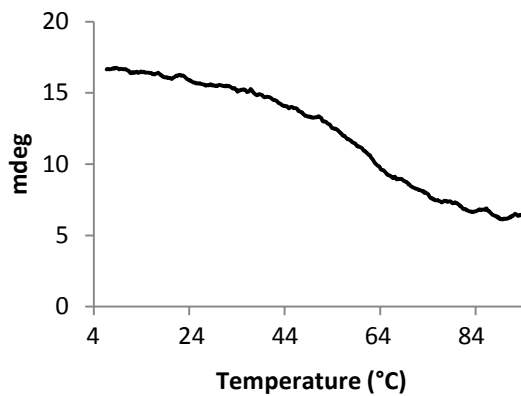
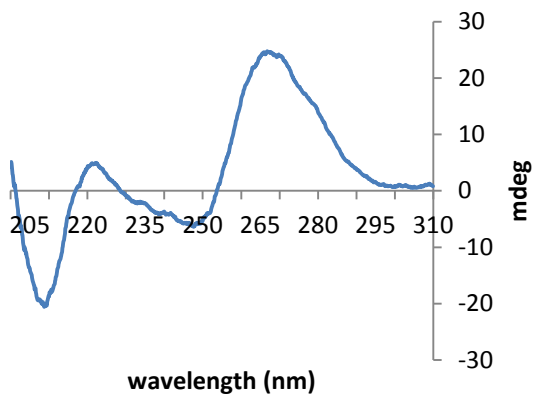


Figure S43. CD (left) and melt (right) of **20**.

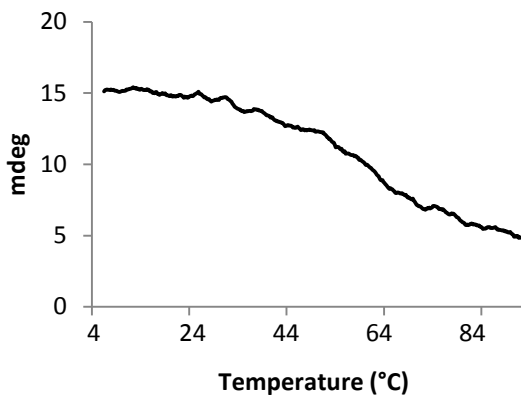
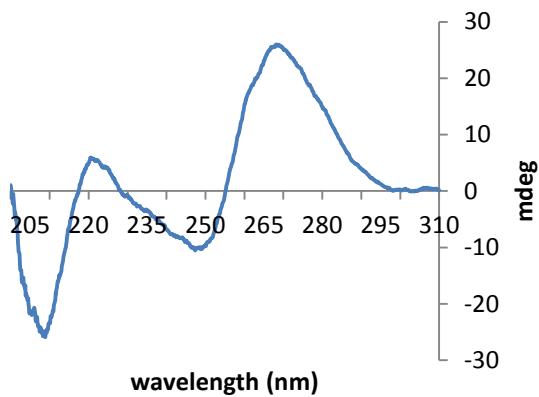


Figure S44. CD (left) and melt (right) of **21**.

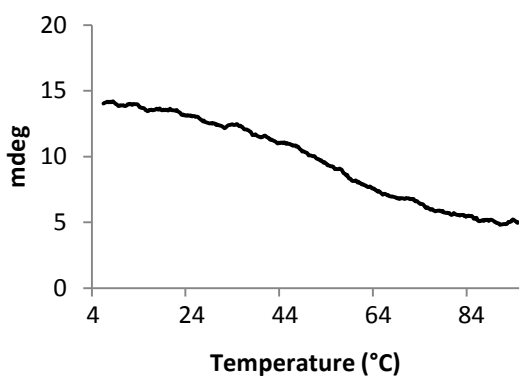
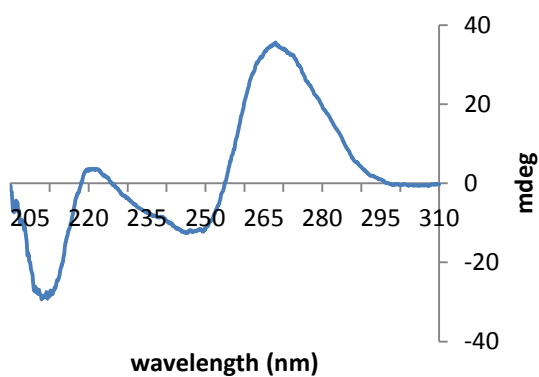


Figure S45. CD (left) and melt (right) of **22**.

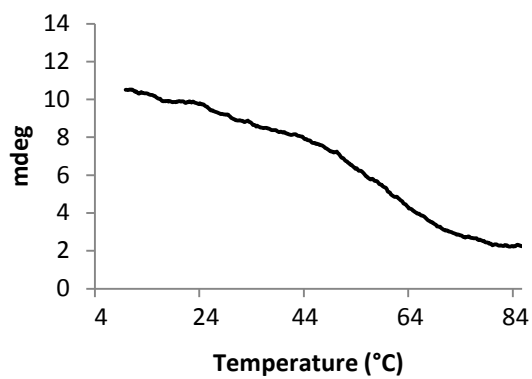
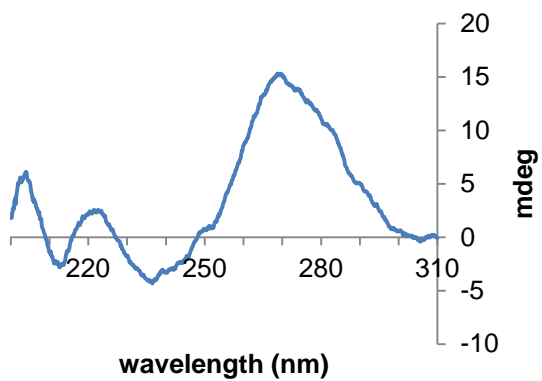


Figure S46. CD (left) and melt (right) of **23**.

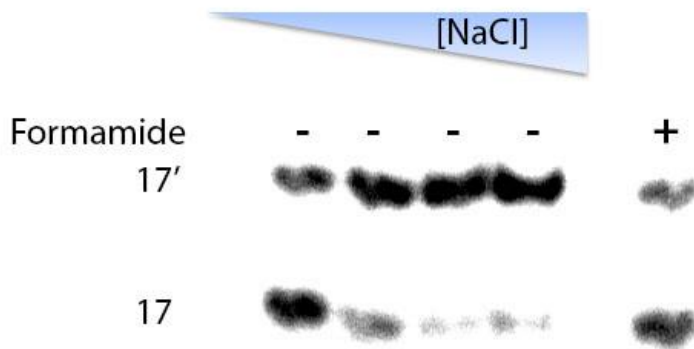


Figure S47. Mobility shift assays for: **17** with increasing [NaCl] at 50, 100, 500, and 1000 mM

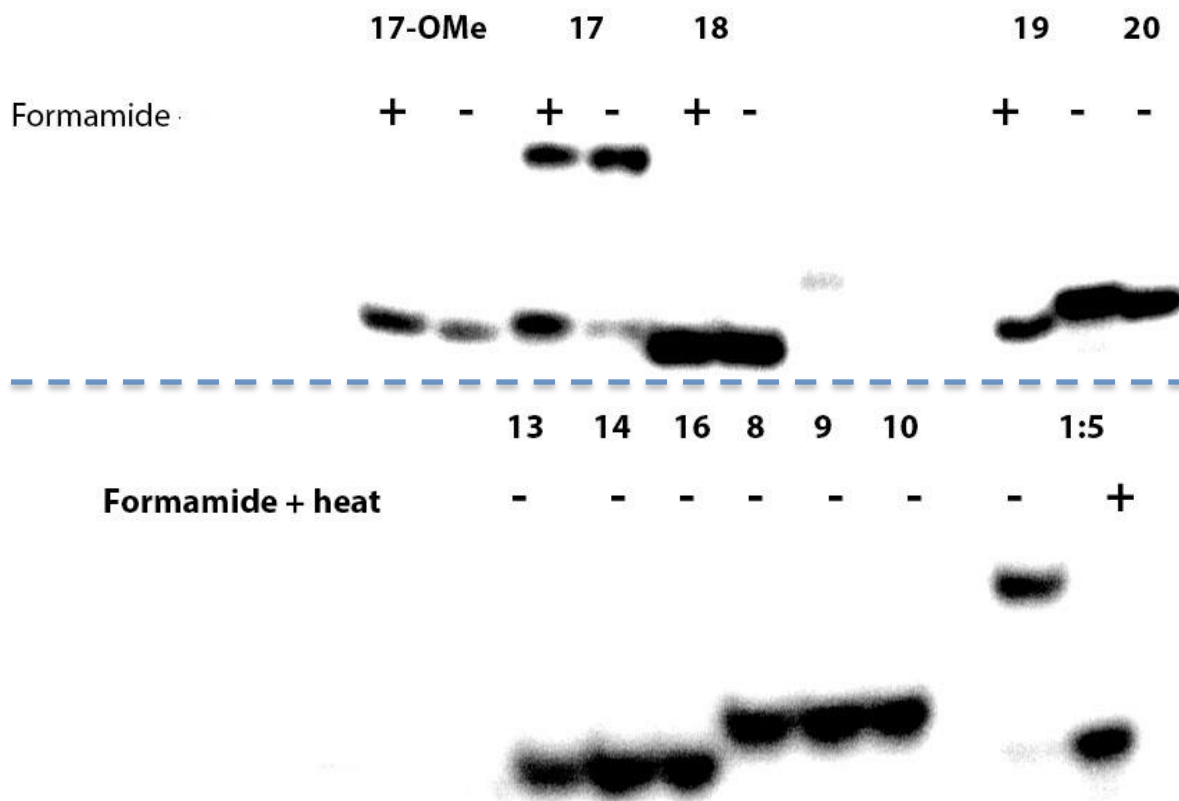


Figure S48. Mobility shift assays for: **17-OMe, 17, 18, 19, 20** w/w/o addn. of formamide (middle); and **13, 14, 16, 8-10** w/o addn. of formamide and control duplex **1:5** w/w/o formamide + heat 75° C (bottom). All gels were carried out in 20 % non-denaturing PAGE.

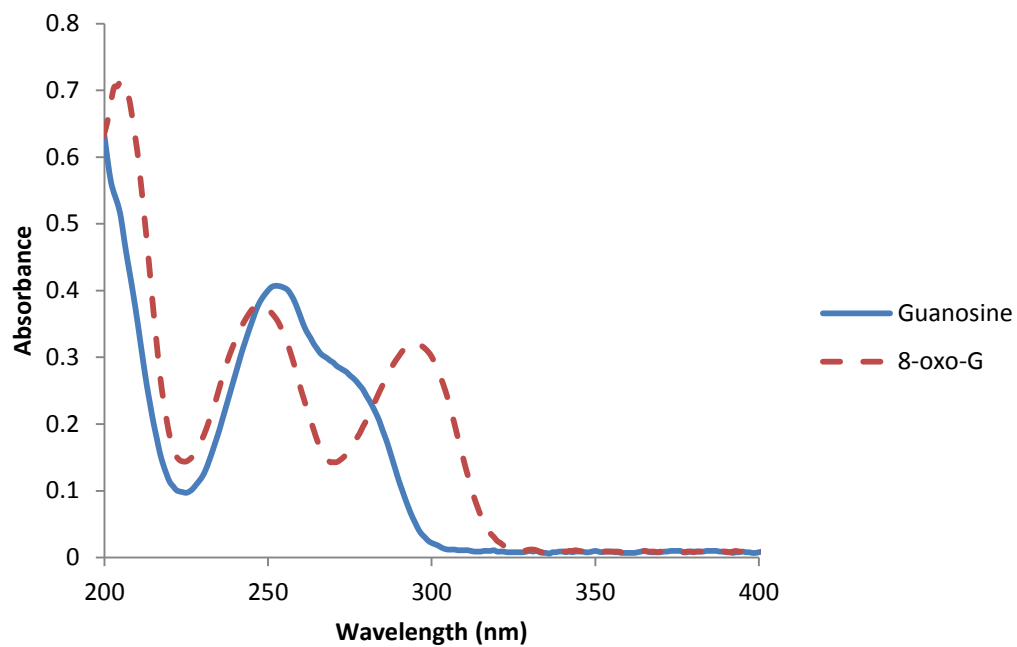


Figure S49. UV-Vis of Guanosine and 8-oxo-G.

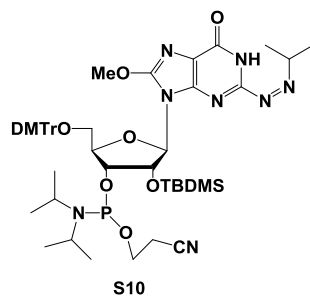


Figure **S50**. Synthesis of **S10** was accomplished by following the known procedures, and the ^1H NMR and ^{31}P NMR chemical shifts matched reference².

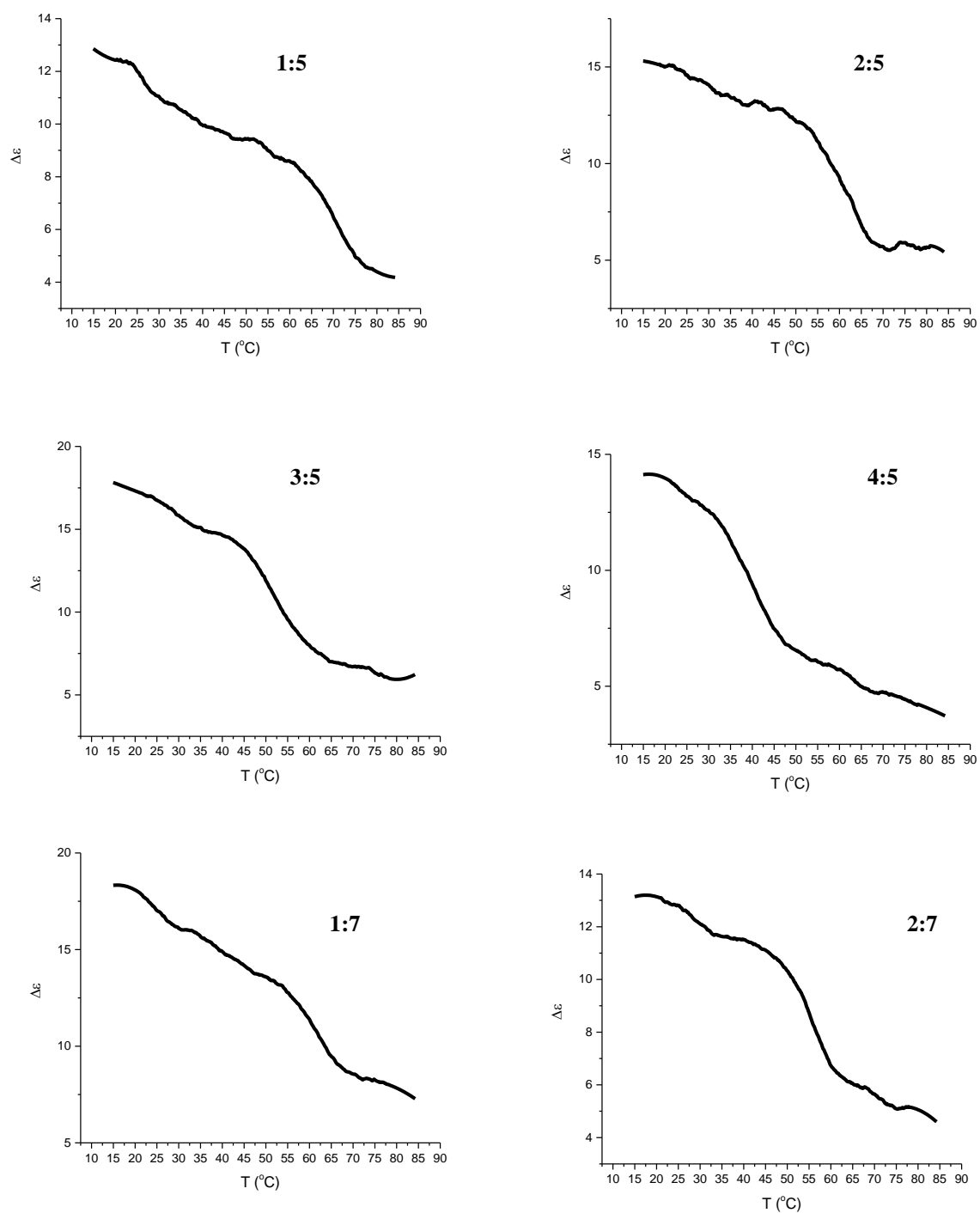


Figure 51. T_m measurements of strands 1:5, 2:5, 3:5, 4:5, 1:7 and 2:7, CD recorded at 270 nm

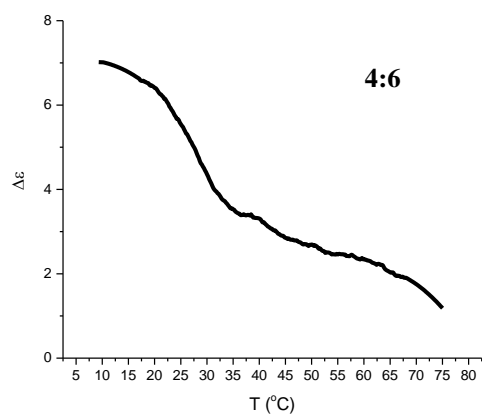
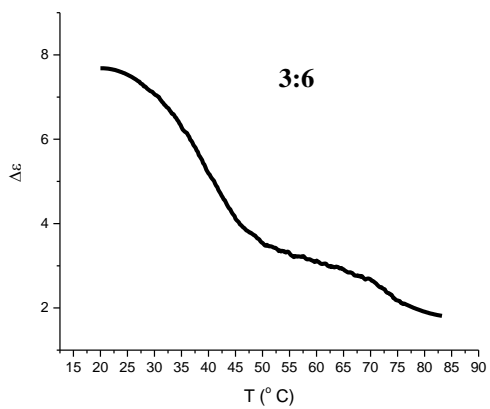
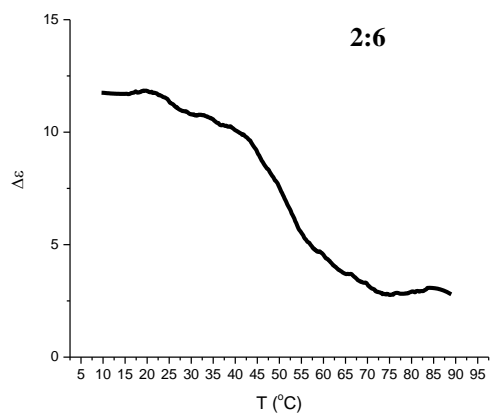
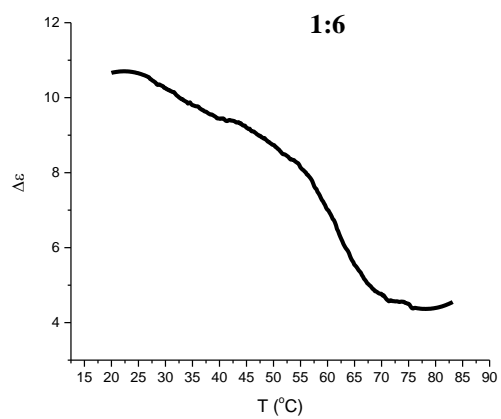


Figure 52. T_m measurements of strands **1:6**, **2:6**, **3:6**, and **4:6**, CD recorded at 270 nm

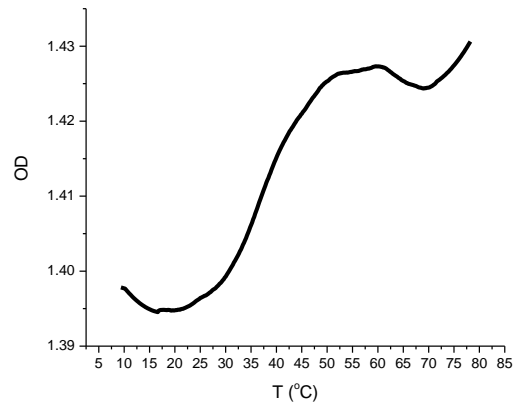
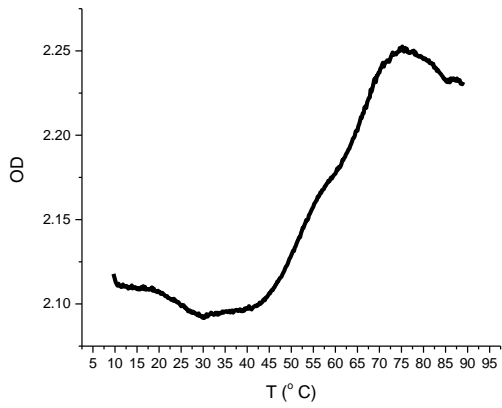
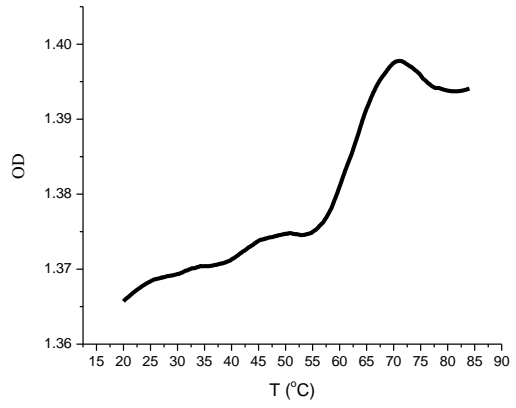
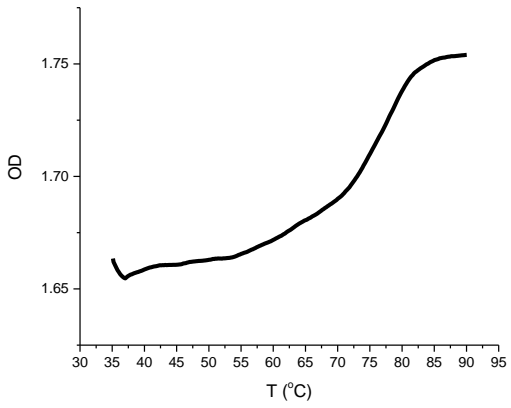


Figure 53. T_m measurements of strands 1:5, 2:5, 3:5, and 4:5, 1:7 OD recorded

REFERENCES

1. Lin, T.S.; Chen, J.C., Ishiguro, K.; Sartorelli, A.C. (1985) 8-Substituted Guanosine and 2'-Deoxyguanosine Derivatives as Potential Inducers of the Differentiation of Friend Erythroleukemia Cells. *J. Med. Chem.*, **28**, 1194-1198.
2. Baranowski, D.S.; Kotkowiak, W.; Kierzek, R.; Pasternak, A. (2015) Hybridization Properties of RNA Containing 8-Methoxyguanosine and 8-Benzyloxyguanosine. *PLoS ONE* **10**(9). doi: 10.1371/journal.pone.0137674.